COMPLEX AVERAGES OF PARTICLE QUANTITIES AND EQUATIONS OF BALANCE

By

ANDREI KOUZNETSOV

A dissertation submitted in partial fulfillment of
the requirements for the degree of

DOCTOR OF PHILOSOPHY

WASHINGTON STATE UNIVERSITY
Department of Mathematics

MAY 2010

To the Faculty of Washington State University:

The members of the Committee appointed to examine the dissertation of ANDREI KOUZNETSOV find it satisfactory and recommend that it be accepted

Alex Panchenko, Ph.D., Chair

Robert H. Dillon, Ph.D.

V.S. Manoranjan, Ph.D.

COMPLEX AVERAGES OF PARTICLE QUANTITIES

AND EQUATIONS OF BALANCE

Abstract

by Andrei Kouznetsov, Ph.D.
Washington State University
May 2010

Chair: Alex Panchenko

We study a new complex continuum quantity $Q^\tau_\eta(t;\boldsymbol{x},\boldsymbol{z})$ and its applications for efficient particle system simulation. Function $Q_\eta(t;\boldsymbol{x},\boldsymbol{z})$ is constructed using both velocities and positions of particles. It carries more information than the standard quantities density, linear momentum, and kinetic energy, and, therefore, it can give better results in various applications. The standard quantities can be derived from $Q^\tau_\eta(t;\boldsymbol{x},\boldsymbol{z})$.

The proposed quantity and its derivatives are bounded independently of the number of particles, and can be used for numerical modeling. Several 1D particle systems are studied using $Q^\tau_\eta(t;\boldsymbol{x},\boldsymbol{z})$, and an approximate closure is presented based on the examples.

Research of $Q^\tau_\eta(t;\boldsymbol{x},\boldsymbol{z})$ can be continued on a 2D example presented in the last chapter. The model in the example describes a so called bistable material. Bistable material is represented by a two-dimensional triangular lattice made of bistable rods. Each rod has two equilibrium lengths, and thus its energy has two equal minima. A rod undergoes a phase transition when its elongation exceeds a critical value. The lattice is subject to a homogeneous strain and is periodic with a sufficiently large period. The effective strain of a periodic element is defined. After phase transitions, the lattice rods are in two different states and lattice strain is inhomogeneous, the Cauchy-Born rule is not applicable. We show that the lattice has a number of deformed *still states* that carry no stresses. These states densely cover a *neutral region* in the space of entries of effective strains. In this region, the minimal energy of the periodic lattice is asymptotically close to zero. The compatibility of the partially transited lattice is studied. We derive compatibility conditions

for lattices and demonstrate a family of compatible lattices (strips) that densely covers the flat bottom region. Under an additional assumption of the small difference of two equilibrium lengths, we demonstrate that the still structures continuously vary with the effective strain and prove a linear dependence of the average strain on the concentration of transited rods.

Contents

List of Figures

Dedication

This thesis is dedicated to my parents and wife who
provided the support without which this
work would have been impossible.

CHAPTER ONE

INTRODUCTION

1.1 Motivation

Modeling a large array of particles becomes computationally infeasible as the size of the array increases along with the number of equations that describe inter-particle connections. In a large array of particles we can not analyze a single particle, but instead we look at certain characteristics of particles. We consider a large array of particles as a set of smooth functions that describe the system. If the functions have certain smoothness that does not depend on the number of particles, then the functions can be approximated by a discrete set of values at nodes of a grid.

In some sense we have two different worlds in our model. The first world is a micro-world that distinguishes single particles. The second world is a macro-world that does not distinguish particles, but it has certain laws and constitutive equations. We want to extract those laws and constitutive equations from the micro-world that is given in terms of particles and their properties.

In the view of the assumptions above, the following question arises. What are the right quantities that give us all necessary information for modeling and analysis? First of all, we would like to have such quantities as density, linear momentum, etc. at every node of our grid. Second, we need to be able to have an evolution law for the system in terms of those quantities.

In this work we propose certain quantities that partially satisfy both requirements: the proposed quantities can be used to obtain the density and linear momentum, also an approximate closed form equation is proposed with an algorithm to compute the evolution of the system.

1.2 Discrete mathematical problem

Consider a system of N identical particles of mass m_N that have no size. We will assume that during the observation all particles have no angular momentum and are located in a bounded domain Ω of the d-dimensional space $\mathbb{R}^d$, $d = 1, 2, 3$. The number of particles N is assumed to be very large and our goal is to obtain asymptotic behavior as $N \to \infty$. The positions $\boldsymbol{q}_j(t)$ and velocities $\boldsymbol{v}_j(t)$

of particles $j = 1, 2, \ldots, N$ satisfy a system of Newton equations

$$\begin{cases} \dot{\boldsymbol{q}}_j(t) = \boldsymbol{v}_j(t), \\ m_N \dot{\boldsymbol{v}}_j(t) = \boldsymbol{f}_j(t) + \boldsymbol{f}_j^{(\text{ext})}(t) \end{cases} \tag{1.1}$$

with some given initial values $\boldsymbol{q}_j(0)$ and $\boldsymbol{v}_j(0)$. Here $\boldsymbol{f}_j^{(\text{ext})}$ denotes external forces, such as gravity and forces enforcing boundary constraints. The interparticle forces are assumed to be of the form

$$\boldsymbol{f}_j = \sum_{k=1}^{N} \boldsymbol{f}_{jk}, \qquad \boldsymbol{f}_{jj} = 0 \tag{1.2}$$

where $\boldsymbol{f}_{jk}$ are pair interaction conservative forces generated by a finite range potential U_N:

$$\boldsymbol{f}_{jk} = -\nabla U_N(\boldsymbol{q}_k(t) - \boldsymbol{q}_j(t)), \quad \text{for } k \neq j \tag{1.3}$$

System (1.1) describes behavior of an array of particles. This behavior strongly depends on the initial conditions $\boldsymbol{q}_j(0)$, $\boldsymbol{v}_j(0)$, and the potential U_N.

1.3 Scaling

Since we are interested in the asymptotic behavior of system (1.1), all quantities of the system should be properly scaled as $N \to \infty$. To define the scaling consider the structure on Figure 1.1. Particles in this structure are uniformly distributed in the cube and each non-boundary particle has 6 interacting neighbors.

As $N \to \infty$ the structure on Figure 1.1 should have a constant mass and a potential energy bounded by a constant independent of N. One way to satisfy these requirements is to define

$$m_N = \frac{M}{N}$$

to ensure that the total mass of the whole system is M, and define

$$U_N(\boldsymbol{x}) = \frac{1}{N} U(N^{\frac{1}{d}} \boldsymbol{x}) = \frac{u(N^{\frac{1}{d}} \|\boldsymbol{x}\|_2)}{N}$$

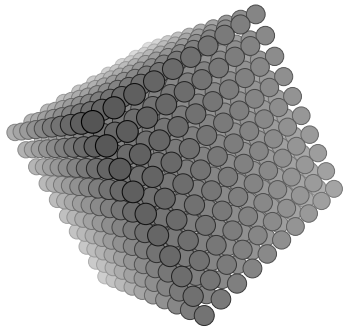

Figure 1.1: Particles packed in a cube

for some function $u : \mathbb{R} \to \mathbb{R}$, $\operatorname{supp} u \subset (0, r)$, so that if we cut the cube, the normal component of the total force is proportional to the area of the section. In the definition of the force we can see that the vector of the force between two interacting particles and the vector connecting the interacting particles are collinear.

For formal explanation define a parameter $\varepsilon = N^{-1/d}$ and suppose that $N \geq N_0$. Then the total mass of the system is M

$$\sum_{j=1}^{N} m_N = \sum_{j=1}^{N} \frac{M}{N} = M$$

and the potential energy $\mathcal{U}_N$ of the system is

$$\mathcal{U}_N = \frac{1}{2} \sum_{j=1}^{N} \sum_{k=1}^{N} U_N(\boldsymbol{q}_j - \boldsymbol{q}_k) = \frac{1}{2} \frac{1}{N} \sum_{j=1}^{N} \sum_{k=1}^{N} U\left(\frac{\boldsymbol{q}_j - \boldsymbol{q}_k}{\varepsilon}\right). \tag{1.4}$$

If we neglect the particles on the edge of the cube, then for the structure on Figure 1.1 the expression for the potential energy will be

$$\mathcal{U}_N = \frac{1}{2} \frac{1}{N} \sum_{j=1}^{N} 6U^\star = \frac{6U^\star}{2}$$

where $U^\star$ is the potential of the link between two neighbors (all neighbors in the cube have the same distance). Hence, the potential energy of the structure does not depend on N. For all other structures we are going to use the same scaling.

The force $\boldsymbol{f}_{jk}$ of interaction between particles j and k, acting on $\boldsymbol{q}_j$ is

$$\boldsymbol{f}_{jk} = -\frac{1}{N\varepsilon}\nabla_{\boldsymbol{x}} U\left(\frac{\boldsymbol{q}_j - \boldsymbol{q}_k}{\varepsilon}\right). \tag{1.5}$$

Scaled as above, system (1.1) becomes

$$\begin{cases} \dot{\boldsymbol{q}}_j(t) = \boldsymbol{v}_j(t), \\ M\dot{\boldsymbol{v}}_j(t) = -\dfrac{1}{\varepsilon}\displaystyle\sum_{k=1}^{N} \nabla_{\boldsymbol{x}} U\left(\frac{\boldsymbol{q}_j - \boldsymbol{q}_k}{\varepsilon}\right) \end{cases} \tag{1.6}$$

In system 1.6 we are interested in the case when $\varepsilon \to 0$.

CHAPTER TWO
LITERATURE REVIEW

Throughout the whole history of our civilization people were trying to understand the world around us. One of the main problems was to explain properties of surrounding objects. People asked themselves why a rock was solid, but water was liquid. Among many different explanations there was one that is used today. This explanation is based on the idea that every material consists of discrete units. The earliest references of this concept date back to ancient India in the 6-th century BCE. In approximately 450 BCE Democritus introduced the term "atomos" which meant the smallest indivisible particle of matter. All those early theories were purely theoretical and were based on philosophy. People believed that properties of a single particle determined properties of a material. A mixture of particles may have different properties depending on the proportions and the nature of the mixing materials.

The question that is still open these days is how we can predict properties of a material using the properties of its particles. One can ask why we want to predict instead of just conducting an experiment. The answer is that today it would be faster and cheaper to use a computer to predict the results if we have a right model that is computationally cheap and accurate.

Many people work on models that can describe behavior and properties of materials. Those models differ by accuracy, the materials that can be modeled by those models, computational cost, complexity of implementation, etc. The main two approaches in modeling are discrete and continuous.

Discrete model assumes that one will work with a system of interacting units. The number of the units can be very large depending on the scale of the problem. If the system becomes large, then usually it becomes too hard to solve this system accurately. However, upon solving the system of equations, one gets information about every unit in his system.

Continuous models employ the fact that in our real life we do not want to know about every discrete unit (atom, molecule, etc.) in our material. Instead, we need some macro characteristics. Moreover, usually, it is assumed that these characteristics are continuous functions of time and space.

There are two different approaches to construct a continuous models. One approach tries to use every particle in equations and then simplify the equations using some a priori information (deterministic mechanics). The other approach does not require information about all particles, but instead it uses probability distribution for model descriptions (statistical mechanics [16, 11]).

Statistical mechanics provides a framework for relating the microscopic properties of discrete units to the macroscopic properties of materials. It was born in 1870 with the work of Austrian physicist Ludwig Boltzmann. The main problem in statistical thermodynamics is to determine the distribution of a given amount of energy E over N identical systems [16]. The goal of statistical mechanics is to relate the measurable macroscopic properties of materials to the properties of the particles. One of the main requirements of the statistical mechanics is having a huge number of particles in the system.

The first models of continuum deterministic mechanics were formulated by the French mathematician Augustin Louis Cauchy in the 19th century, but research in the area continues today. Modeling an object as a continuum assumes that the substance of the object completely fills the space that it occupies, therefore, we ignore the fact that matter consists of atoms. However, on length scales much greater than inter-atomic distances, such models are highly accurate. Fundamental physical laws such as the conservation of mass, the conservation of momentum, and the conservation of energy may be applied to such models to derive differential equations describing the behavior of such objects, and some information about the particular material studied is added through a constitutive relation (for example see [23]), a relation between two physical quantities that is specific to a material or substance, and approximates the response of that material to external forces.

There are many attempts to derive a closed system of macroscopic characteristics that will describe the properties of materials based on the properties of the discrete units of the materials. But so far there is no such theory that can describe all possible cases.

A good example of the work that introduces a continuous structure of a material using the discrete units of this material was done by A. I. Murdoch and D. Bedeaux [13, 14]. In 1994 authors presented exact continuum forms of balance [13]. All macro quantities were obtained using weighted averages of microscopic quantities. The weighting function was a continuous function that determined the smoothness of all macroscopic characteristics. In that paper they also discussed

the choice of that function. Later, in 2007 A. Ian Murdoch compared different definitions and derivations of the Cauchy stress tensor and suggested an approach in nanoscale systems [14].

The idea of the current work is to propose some new macro characteristics that carry more information than the standard averages like the density, linear momentum, energy, etc. These new averages are the main difference of this work from the previous works. It is shown that using the new proposed averages one can find a closed form equation for simple systems like ideal gas. The new averages still do not carry all the information that is needed to construct a closed system for an arbitrary case, but using some approximate identities we can construct an algorithm that will be expected to produce better results than using the standard averages.

CHAPTER THREE

GENERATING FUNCTIONS

3.4 Classical space-time averages

We work with space-time averaging pioneered by Noll [23], and further developed by Hardy [10] and later Murdoch and Bedeaux [13, 14]. In this section we briefly recall the basic points of the method and introduce the relevant notation.

Choose smooth functions $\psi(\boldsymbol{x}) \geq 0$, $\boldsymbol{x} \in \mathbb{R}^d$, and $\phi(t) \geq 0$, $t \in \mathbb{R}$. These functions will be used to generate spatial and time averages, respectively. We will assume that the functions are normalized

$$\int_{\mathbb{R}^d} \psi(\boldsymbol{x}) d\boldsymbol{x} = 1 \quad \text{and} \quad \int_{\mathbb{R}} \phi(t) dt = 1$$

and decay sufficiently fast as $|\boldsymbol{x}| \to \infty$ and $|t| \to \infty$. Many choices of ψ and ϕ are possible, however for practical use it is reasonable to use smooth functions with bounded support.

Define the following new functions

$$\psi_\eta(\boldsymbol{x}) = \eta^{-d} \psi\left(\frac{\boldsymbol{x}}{\eta}\right) \quad \text{and} \quad \phi^\tau(t) = \frac{1}{\tau} \phi\left(\frac{t}{\tau}\right)$$

The new functions ψ_η and ϕ_τ form nets (generalized sequences) converging to delta functions as $\eta \to 0$ and $\tau \to 0$ in the space and time domains, respectively. Using these functions define the common continuum mechanical quantities:

1. density

$$\rho_\eta(t; \boldsymbol{x}) = \frac{M}{N} \sum_{j=1}^{N} \psi_\eta(\boldsymbol{x} - \boldsymbol{q}_j(t)), \tag{3.7}$$

2. linear momentum

$$\boldsymbol{p}_\eta(t; \boldsymbol{x}) = \frac{M}{N} \sum_{j=1}^{N} \boldsymbol{v}_j(t) \psi_\eta(\boldsymbol{x} - \boldsymbol{q}_j(t)), \tag{3.8}$$

3. kinetic energy

$$K_\eta(t;\boldsymbol{x}) = \frac{1}{2}\frac{M}{N}\sum_{j=1}^{N} \boldsymbol{v}_j(t)\cdot\boldsymbol{v}_j(t)\psi_\eta(\boldsymbol{x}-\boldsymbol{q}_j(t)). \tag{3.9}$$

Differentiating $\rho_\eta(t,\boldsymbol{x})$ and $\boldsymbol{p}_\eta(t,\boldsymbol{x})$ with respect to time and using the system (1.1) one can obtain the balance equations:

$$\partial_t\rho_\eta(t,\boldsymbol{x}) + \mathrm{div}_{\boldsymbol{x}}\,\boldsymbol{p}_\eta(t,\boldsymbol{x}) = 0, \tag{3.10}$$

and

$$\partial_t\boldsymbol{p}_\eta(t,\boldsymbol{x}) = \mathrm{div}_{\boldsymbol{x}}\,\boldsymbol{T}_\eta(t,\boldsymbol{x}) \tag{3.11}$$

The stress $\boldsymbol{T}_\eta(t,\boldsymbol{x})$ can be written as the difference (see [14]):

$$\boldsymbol{T}_\eta(t,\boldsymbol{x}) = \boldsymbol{F}_\eta(t,\boldsymbol{x}) - \boldsymbol{D}_\eta(t,\boldsymbol{x}) \tag{3.12}$$

where

$$\boldsymbol{F}_\eta(t,\boldsymbol{x}) = -\frac{1}{2}\sum_{j=1}^{N}\sum_{k=1}^{N}\boldsymbol{f}_{jk}\otimes(\boldsymbol{q}_j-\boldsymbol{q}_k)\int_0^1\psi_\eta(\boldsymbol{x}-s\boldsymbol{q}_j-(1-s)\boldsymbol{q}_k))ds \tag{3.13}$$

$$\boldsymbol{D}_\eta(t,\boldsymbol{x}) = \frac{M}{N}\sum_{j=1}^{N}\boldsymbol{v}_j\otimes\boldsymbol{v}_j\psi_\eta(\boldsymbol{q}_j-\boldsymbol{x}) \tag{3.14}$$

and symbol "$\otimes$" denotes the tensor product of two vectors:

$$\boldsymbol{a}\otimes\boldsymbol{b} = \boldsymbol{a}\boldsymbol{b}^T, \qquad (\boldsymbol{a}\otimes\boldsymbol{b})_{i,j} = \boldsymbol{a}_i\boldsymbol{b}_j$$

Observe that

$$K_\eta(t,\boldsymbol{x}) = \frac{1}{2}\,\mathrm{Tr}\,\boldsymbol{D}_\eta(t,\boldsymbol{x})$$

Next, for spatial averaged quantities we can define time averages:

$$\rho_\eta^\tau(t,\boldsymbol{x}) = \int_{\mathbb{R}} \rho_\eta(s,\boldsymbol{x})\phi^\tau(t-s)ds \tag{3.15}$$

$$\boldsymbol{p}_\eta^\tau(t,\boldsymbol{x}) = \int_{\mathbb{R}} \boldsymbol{p}_\eta(s,\boldsymbol{x})\phi^\tau(t-s)ds \tag{3.16}$$

$$\boldsymbol{T}_\eta^\tau(t,\boldsymbol{x}) = \int_{\mathbb{R}} \boldsymbol{T}_\eta(s,\boldsymbol{x})\phi^\tau(t-s)ds \tag{3.17}$$

$$\boldsymbol{D}_\eta^\tau(t,\boldsymbol{x}) = \int_{\mathbb{R}} \boldsymbol{D}_\eta(s,\boldsymbol{x})\phi^\tau(t-s)ds \tag{3.18}$$

$$\boldsymbol{F}_\eta^\tau(t,\boldsymbol{x}) = \int_{\mathbb{R}} \boldsymbol{F}_\eta(s,\boldsymbol{x})\phi^\tau(t-s)ds \tag{3.19}$$

It is easy to see that equations (3.11) and (3.12) can be written for the time averages as

$$\partial_t \boldsymbol{p}_\eta^\tau(t,\boldsymbol{x}) = \operatorname{div}_{\boldsymbol{x}} \boldsymbol{T}_\eta^\tau(t,\boldsymbol{x}) \tag{3.20}$$

$$\boldsymbol{T}_\eta^\tau(t,\boldsymbol{x}) = \boldsymbol{F}_\eta^\tau(t,\boldsymbol{x}) - \boldsymbol{D}_\eta^\tau(t,\boldsymbol{x}) \tag{3.21}$$

Our goal is to describe the evolution of the time-space averages without description of all particles.

3.5 Generating function

Let us introduce the generating function

$$Q_\eta(t;\boldsymbol{x},\boldsymbol{z}) = \frac{M}{N}\sum_{j=1}^{N} e^{i\boldsymbol{v}_j(t)\cdot\boldsymbol{z}}\psi_\eta(\boldsymbol{x}-\boldsymbol{q}_j(t)) \tag{3.22}$$

where $\boldsymbol{q}_j \in \Omega$ is the position of particle j and $\boldsymbol{v}_j$ is the velocity of particle j (Ω is a bounded subset of $\mathbb{R}^d$). The new variable $\boldsymbol{z} \in \mathbb{R}^d$ is an axillary variable that helps extract some certain information about particle velocities from $Q_\eta(t;\boldsymbol{x},\boldsymbol{z})$.

First, observe that the quantities $\rho_\eta(t,\boldsymbol{x})$, $\boldsymbol{p}_\eta(t,\boldsymbol{x})$, and $\boldsymbol{D}_\eta(t,\boldsymbol{x})$ can be obtained from $Q_\eta(t,\boldsymbol{x},\boldsymbol{z})$

through the following equations

$$\begin{aligned}
\rho_\eta(t,\boldsymbol{x}) &= Q_\eta(t;\boldsymbol{x},0) = \frac{M}{N}\sum_{j=1}^{N}\psi(\boldsymbol{x}-\boldsymbol{q}_j(t)) \\
\boldsymbol{p}_\eta(t,\boldsymbol{x}) &= -i\nabla_{\boldsymbol{z}}Q_\eta(t;\boldsymbol{x},0) = \frac{M}{N}\sum_{j=1}^{N}\boldsymbol{v}_j(t)\psi_\eta(\boldsymbol{x}-\boldsymbol{q}_j(t)) \\
\boldsymbol{D}_\eta(t,\boldsymbol{x}) &= -\nabla_{\boldsymbol{z}}\nabla_{\boldsymbol{z}}Q_\eta(t;\boldsymbol{x},0) = \frac{M}{N}\sum_{j=1}^{N}\boldsymbol{v}_j(t)\otimes\boldsymbol{v}_j(t)\psi_\eta(\boldsymbol{x}-\boldsymbol{q}_j(t))
\end{aligned}$$

This means that the named above functions can be substituted for the function $Q_\eta(t,\boldsymbol{x},\boldsymbol{z})$ in computations. Next, by direct differentiation we find that

$$\partial_t Q_\eta(t;\boldsymbol{x},\boldsymbol{z}) = i\boldsymbol{z}\cdot\boldsymbol{f}_\eta(t;\boldsymbol{x},\boldsymbol{z}) + i\,\mathrm{div}_{\boldsymbol{x}}\,\nabla_{\boldsymbol{z}}Q_\eta(t;\boldsymbol{x},\boldsymbol{z}) \tag{3.23}$$

where the term $\boldsymbol{f}_\eta(t;\boldsymbol{x},\boldsymbol{z})$ is

$$\boldsymbol{f}_\eta(t;\boldsymbol{x},\boldsymbol{z}) = M\frac{1}{N}\sum_{j=1}^{N}\dot{\boldsymbol{v}}_j e^{i\boldsymbol{v}_j(t)\cdot\boldsymbol{z}}\psi_\eta(\boldsymbol{x}-\boldsymbol{q}_j(t)) \tag{3.24}$$

and can be rewritten using (1.6) as

$$\boldsymbol{f}_\eta(t;\boldsymbol{x},\boldsymbol{z}) = \frac{1}{N}\sum_{j=1}^{N}\left\{-\frac{1}{\varepsilon}\sum_{k=1}^{N}\nabla U\left(\frac{\boldsymbol{q}_j(t)-\boldsymbol{q}_k(t)}{\varepsilon}\right)\right\}e^{i\boldsymbol{v}_j(t)\cdot\boldsymbol{z}}\psi_\eta(\boldsymbol{x}-\boldsymbol{q}_j(t)) \tag{3.25}$$

Theorem 1. *For function $Q_\eta(t;\boldsymbol{x},\boldsymbol{z})$ we have the following estimates*

1. $|Q_\eta(t;\boldsymbol{x},\boldsymbol{z})| \le \rho_\eta(t;\boldsymbol{x}) \le M\|\psi_\eta\|_{W^0_\infty(\mathbb{R}^d)}$
2. $\|\nabla_{\boldsymbol{x}}Q_\eta(t;\boldsymbol{x},\boldsymbol{z})\|_2 \le M\|\psi_\eta\|_{W^1_\infty(\mathbb{R}^d)}$
3. $\|\nabla_{\boldsymbol{z}}Q_\eta(t;\boldsymbol{x},\boldsymbol{z})\|_2 \le \rho_\eta(t;\boldsymbol{x}) + 2K_\eta(t;\boldsymbol{x}) \le (M+2\mathcal{K}(t))\|\psi_\eta\|_{W^0_\infty(\mathbb{R}^d)}$
4. $|\,\mathrm{div}_{\boldsymbol{x}}\,\nabla_{\boldsymbol{z}}Q_\eta(t;\boldsymbol{x},\boldsymbol{z})| \le (M+2\mathcal{K}(t))\|\psi_\eta\|_{W^1_\infty(\mathbb{R}^d)}$

where M is the total mass of the system and $\mathcal{K}(t)$ is the total kinetic energy of the system:

$$\mathcal{K}(t) = \int_{\mathbb{R}^d} K(t;\boldsymbol{x})d\boldsymbol{x} = \sum_{j=1}^{N}\frac{M}{N}\frac{\boldsymbol{v}_j(t)\cdot\boldsymbol{v}_j(t)}{2}$$

Proof. 1. Indeed, using the triangle inequality

$$|Q_\eta(t;\boldsymbol{x},\boldsymbol{z})| = \left| \frac{M}{N} \sum_{j=1}^{N} e^{i\boldsymbol{v}_j(t)\cdot\boldsymbol{z}} \psi_\eta(\boldsymbol{x}-\boldsymbol{q}_j(t)) \right| \leq \frac{M}{N} \sum_{j=1}^{N} \left| e^{i\boldsymbol{v}_j(t)\cdot\boldsymbol{z}} \right| \psi_\eta(\boldsymbol{x}-\boldsymbol{q}_j(t)) = \rho_\eta(t;\boldsymbol{x})$$

Observe that

$$\rho_\eta(t;\boldsymbol{x}) = \frac{M}{N} \sum_{j=1}^{N} \psi_\eta(\boldsymbol{x}-\boldsymbol{q}_j(t)) \leq M \|\psi_\eta\|_{W^0_\infty(\mathbb{R}^d)}$$

2. Next, using the triangle inequality we get

$$\begin{aligned} \|\nabla_{\boldsymbol{x}} Q_\eta(t;\boldsymbol{x},\boldsymbol{z})\|_2 &= \left\| \frac{M}{N} \sum_{j=1}^{N} e^{i\boldsymbol{v}_j(t)\cdot\boldsymbol{z}} \nabla_{\boldsymbol{x}} \psi_\eta(\boldsymbol{x}-\boldsymbol{q}_j(t)) \right\|_2 \\ &\leq \frac{M}{N} \sum_{j=1}^{N} \left| e^{i\boldsymbol{v}_j(t)\cdot\boldsymbol{z}} \right| \|\nabla_{\boldsymbol{x}} \psi_\eta(\boldsymbol{x}-\boldsymbol{q}_j(t))\|_2 \\ &\leq M \|\psi_\eta\|_{W^1_\infty(\mathbb{R}^d)} \end{aligned}$$

3. We have

$$\begin{aligned} \|\nabla_{\boldsymbol{z}} Q_\eta(t;\boldsymbol{x},\boldsymbol{z})\|_2 &= \left\| \frac{M}{N} \sum_{j=1}^{N} i\boldsymbol{v}_j(t) e^{i\boldsymbol{v}_j(t)\cdot\boldsymbol{z}} \psi_\eta(\boldsymbol{x}-\boldsymbol{q}_j(t)) \right\|_2 \\ &\leq \frac{M}{N} \sum_{j=1}^{N} \|\boldsymbol{v}_j(t)\|_2 \psi_\eta(\boldsymbol{x}-\boldsymbol{q}_j(t)) \end{aligned}$$

Using the fact that for all $a \in \mathbb{R}$

$$a < 1 + a^2$$

we conclude that

$$\begin{aligned} \|\nabla_{\boldsymbol{z}} Q_\eta(t;\boldsymbol{x},\boldsymbol{z})\|_2 &< \frac{M}{N} \sum_{j=1}^{N} (1 + \|\boldsymbol{v}_j(t)\|_2^2) \psi_\eta(\boldsymbol{x}-\boldsymbol{q}_j(t)) = \rho_\eta(t;\boldsymbol{x}) + 2K_\eta(t;\boldsymbol{x}) \\ &\leq M \|\psi_\eta\|_{W^0_\infty(\mathbb{R}^d)} + 2\mathcal{K}(t) \|\psi_\eta\|_{W^0_\infty(\mathbb{R}^d)} \\ &\leq (M + 2\mathcal{K}(t)) \|\psi_\eta\|_{W^0_\infty(\mathbb{R}^d)} \end{aligned}$$

4. Consider

$$\begin{aligned}
|\operatorname{div}_{\boldsymbol{x}} \nabla_{\boldsymbol{z}} Q_\eta(t;\boldsymbol{x},\boldsymbol{z})| &= \left| \frac{M}{N} \sum_{j=1}^{N} i e^{i\boldsymbol{v}_j(t)\cdot\boldsymbol{z}} \boldsymbol{v}_j \cdot \nabla_{\boldsymbol{x}} \psi_\eta(\boldsymbol{x}-\boldsymbol{q}_j(t)) \right| \\
&\le \frac{M}{N} \sum_{j=1}^{N} \|\boldsymbol{v}_j(t)\|_2 \|\nabla_{\boldsymbol{x}} \psi_\eta(\boldsymbol{x}-\boldsymbol{q}_j(t))\|_2 \\
&\le \frac{M}{N} \sum_{j=1}^{N} (1+\|\boldsymbol{v}_j(t)\|_2^2) \|\nabla_{\boldsymbol{x}} \psi_\eta(\boldsymbol{x}-\boldsymbol{q}_j(t))\|_2 \\
&\le \frac{M}{N} \sum_{j=1}^{N} \|\nabla_{\boldsymbol{x}} \psi_\eta(\boldsymbol{x}-\boldsymbol{q}_j(t))\|_2 + \frac{M}{N} \sum_{j=1}^{N} \|\boldsymbol{v}_j(t)\|_2^2 \|\nabla_{\boldsymbol{x}} \psi_\eta(\boldsymbol{x}-\boldsymbol{q}_j(t))\|_2 \\
&\le M \|\psi_\eta\|_{W^1_\infty(\mathbb{R}^d)} + 2\mathcal{K}(t) \|\psi_\eta\|_{W^1_\infty(\mathbb{R}^d)} \\
&\le (M+2\mathcal{K}(t)) \|\psi_\eta\|_{W^1_\infty(\mathbb{R}^d)}
\end{aligned}$$

□

Remark 1. *It is possible to find a system that has unbounded force term* $\boldsymbol{f}_\eta(t;\boldsymbol{x},\boldsymbol{z})$ *but bounded* $\rho_\eta(t;\boldsymbol{x})$ *and* $\mathcal{K}(t)$ *as* $N \to \infty$.

Proof. Consider the one dimensional system of N particles with even N (see figure 3.2):

$$q_j = \frac{j + \frac{1}{3}(-1)^{j-1}}{N}, \qquad v_j = \begin{cases} 0 & j \text{ is even} \\ \pi & j \text{ is odd} \end{cases}$$

In this system we have two groups of particles (white and black on Figure 3.2: one group of particles is moving right with a constant velocity, another group has zero velocity.

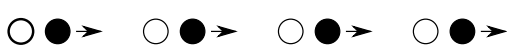

Figure 3.2: Example of a system with unbounded $\boldsymbol{f}(\boldsymbol{x},\boldsymbol{z})$.

For this system of particles we have

$$0 < q_j < 1, \qquad N(q_{j+1}-q_j) = 1 + \frac{2}{3}(-1)^j = \begin{cases} 5/3 & j \text{ is even} \\ 1/3 & j \text{ is odd} \end{cases}$$

Next, pick a smooth function ψ which is equal to a constant A on the interval $[-2,2]$ (see figure

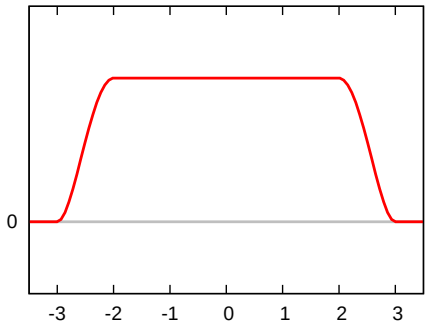

Figure 3.3: An example of ψ.

3.3) and a function U such that

$$\operatorname{supp} \nabla U(x) \subset \left(-\frac{5}{3}, \frac{5}{3}\right), \qquad \nabla U(1/3) = B$$

for some constant $B \neq 0$. Then,

$$\begin{aligned}
\rho_\eta(x) &= \frac{M}{N}\sum_{j=1}^{N}\psi(x-q_j) = \frac{M}{N}\sum_{j=1}^{N} A = MA \\
\mathcal{K} &= \sum_{j=1}^{N}\frac{M}{N}\frac{\boldsymbol{v}_j\cdot\boldsymbol{v}_j}{2} = \frac{M}{2}\frac{\pi^2}{2} \\
f(x,1) &= \frac{1}{N}\sum_{j=1}^{N}\left\{-N^{\frac{1}{d}}\sum_{k=1}^{N}\nabla U((q_j-q_k)N^{\frac{1}{d}})\right\}e^{iv_j\cdot 1}\psi(x-q_j) \\
&= \frac{1}{N}\sum_{j=1}^{N}\left\{-N\sum_{k=1}^{N}\nabla U((q_j-q_k)N)\right\}(-1)^j A \\
&= \frac{1}{N}\sum_{j=1}^{N} NB(-1)^j(-1)^j A \\
&= ABN
\end{aligned}$$

Therefore, $f(x,1) \to \infty$ as $N \to \infty$. □

Theorem 2. *Define new time averaged quantities*

$$Q_\eta^\tau(t;\boldsymbol{x},\boldsymbol{z}) = \int_{-\infty}^{+\infty} Q_\eta(s;\boldsymbol{x},\boldsymbol{z})\phi^\tau(t-s)ds, \qquad \boldsymbol{f}_\eta^\tau(t;\boldsymbol{x},\boldsymbol{z}) = \int_{-\infty}^{+\infty} \boldsymbol{f}_\eta(s;\boldsymbol{x},\boldsymbol{z})\phi^\tau(t-s)ds$$

Then the following statements are true

1. *Functions Q_η^τ and $\boldsymbol{f}_\eta^\tau$ satisfy differential equation (3.23)*
2. $|Q_\eta^\tau(\boldsymbol{x},\boldsymbol{z})| \le M\|\psi_\eta\|_{W_\infty^0(\mathbb{R}^d)}$
3. $\|\nabla_{\boldsymbol{x}} Q_\eta^\tau(t;\boldsymbol{x},\boldsymbol{z})\|_2 \le M\|\psi_\eta\|_{W_\infty^1(\mathbb{R}^d)}$
4. $\|\nabla_{\boldsymbol{z}} Q_\eta^\tau(t;\boldsymbol{x},\boldsymbol{z})\|_2 \le (M+2\mathcal{K}(t))\|\psi_\eta\|_{W_\infty^0(\mathbb{R}^d)}$
5. $|\operatorname{div}_{\boldsymbol{x}} \nabla_{\boldsymbol{z}} Q_\eta^\tau(t;\boldsymbol{x},\boldsymbol{z})| \le (M+2\mathcal{K}(t))\|\psi_\eta\|_{W_\infty^1(\mathbb{R}^d)}$
6. $|\partial_t Q_\eta^\tau(t;\boldsymbol{x},\boldsymbol{z})| \le M\|\psi_\eta\|_{W_\infty^0(\mathbb{R}^d)}\|\phi^\tau\|_{W_1^1(\mathbb{R}^d)}$
7. $|\boldsymbol{z}\cdot\boldsymbol{f}_\eta^\tau(t;\boldsymbol{x},\boldsymbol{z})| \le (M+2\mathcal{K}(t))\|\psi_\eta\|_{W_\infty^1(\mathbb{R}^d)} + M\|\psi_\eta\|_{W_\infty^0(\mathbb{R}^d)}\|\phi^\tau\|_{W_1^1(\mathbb{R}^d)}$

Proof. 1. Consider

$$\partial_t Q_\eta^\tau(t;\boldsymbol{x},\boldsymbol{z}) = \frac{d}{dt}\int_{-\infty}^{+\infty} Q_\eta(s;\boldsymbol{x},\boldsymbol{z})\phi^\tau(t-s)ds = \int_{-\infty}^{+\infty} Q_\eta(s;\boldsymbol{x},\boldsymbol{z})D_t\phi^\tau(t-s)ds$$

Using the fact that function ϕ has bounded support, we find

$$\partial_t Q_\eta^\tau(t;\boldsymbol{x},\boldsymbol{z}) = \int_{-\infty}^{+\infty} \frac{d}{ds}\{Q_\eta(s;\boldsymbol{x},\boldsymbol{z})\}\phi^\tau(t-s)ds$$

Since function $Q_\eta(t;\boldsymbol{x},\boldsymbol{z})$ satisfies (3.23), we find

$$\partial_t Q_\eta^\tau(t;\boldsymbol{x},\boldsymbol{z}) = i\boldsymbol{z}\cdot\boldsymbol{f}^\tau(t;\boldsymbol{x},\boldsymbol{z}) + i\operatorname{div}_{\boldsymbol{x}}\nabla_{\boldsymbol{z}} Q_\eta^\tau(t;\boldsymbol{x},\boldsymbol{z})$$

2. By the definition of Q^τ we have

$$|Q_\eta^\tau(t;\boldsymbol{x},\boldsymbol{z})| = \left|\int_{-\infty}^{+\infty} Q_\eta(s;\boldsymbol{x},\boldsymbol{z})\phi^\tau(t-s)ds\right| \le \int_{-\infty}^{+\infty} |Q_\eta(\boldsymbol{x},\boldsymbol{z})|\phi^\tau(t-s)ds$$

Using Theorem 1 we find

$$|Q_\eta^\tau(t;\boldsymbol{x},\boldsymbol{z})| \le M\|\psi_\eta\|_{W_\infty^0(\mathbb{R}^d)}\int_{-\infty}^{+\infty}\phi^\tau(t-s)ds = M\|\psi_\eta\|_{W_\infty^0(\mathbb{R}^d)}$$

3. By the definition of Q^τ we have

$$\|\nabla_{\boldsymbol{x}} Q_\eta^\tau(t;\boldsymbol{x},\boldsymbol{z})\|_2 = \left\| \int_{-\infty}^{+\infty} \nabla_{\boldsymbol{x}} Q_\eta(s;\boldsymbol{x},\boldsymbol{z}) \phi^\tau(t-s) ds \right\|_2 \leq \int_{-\infty}^{+\infty} \|\nabla_{\boldsymbol{x}} Q_\eta(s;\boldsymbol{x},\boldsymbol{z})\|_2 \phi^\tau(t-s) ds$$

Using Theorem 1 we find

$$\|\nabla_{\boldsymbol{x}} Q_\eta^\tau(t;\boldsymbol{x},\boldsymbol{z})\|_2 \leq M \|\psi_\eta\|_{W^1_\infty(\mathbb{R}^d)} \int_{-\infty}^{+\infty} \phi^\tau(t-s) ds = M \|\psi_\eta\|_{W^1_\infty(\mathbb{R}^d)}$$

4. By the definition of Q^τ we have

$$\|\nabla_{\boldsymbol{z}} Q_\eta^\tau(t;\boldsymbol{x},\boldsymbol{z})\|_2 = \left\| \int_{-\infty}^{+\infty} \nabla_{\boldsymbol{z}} Q_\eta(s;\boldsymbol{x},\boldsymbol{z}) \phi^\tau(t-s) ds \right\|_2 \leq \int_{-\infty}^{+\infty} \|\nabla_{\boldsymbol{z}} Q_\eta(s;\boldsymbol{x},\boldsymbol{z})\|_2 \phi^\tau(t-s) ds$$

Using Theorem 1 we find

$$\begin{aligned} \|\nabla_{\boldsymbol{z}} Q_\eta^\tau(t;\boldsymbol{x},\boldsymbol{z})\|_2 &\leq (M + 2\mathcal{K}(t)) \|\psi_\eta\|_{W^0_\infty(\mathbb{R}^d)} \int_{-\infty}^{+\infty} \phi^\tau(t-s) ds \\ &= (M + 2\mathcal{K}(t)) \|\psi_\eta\|_{W^0_\infty(\mathbb{R}^d)} \end{aligned}$$

5. By the definition of Q^τ we have

$$|\operatorname{div}_{\boldsymbol{x}} \nabla_{\boldsymbol{z}} Q_\eta^\tau(t;\boldsymbol{x},\boldsymbol{z})| = \left| \int_{-\infty}^{+\infty} \nabla_{\boldsymbol{z}} Q_\eta(s;\boldsymbol{x},\boldsymbol{z}) \phi^\tau(t-s) ds \right| \leq \int_{-\infty}^{+\infty} |\operatorname{div}_{\boldsymbol{x}} \nabla_{\boldsymbol{z}} Q_\eta(s;\boldsymbol{x},\boldsymbol{z})| \phi^\tau(t-s) ds$$

Using Theorem 1 we find

$$|\operatorname{div}_{\boldsymbol{x}} \nabla_{\boldsymbol{x}} Q_\eta^\tau(t;\boldsymbol{x},\boldsymbol{z})| \leq (M + 2\mathcal{K}(t)) \|\psi_\eta\|_{W^1_\infty(\mathbb{R}^d)} \int_{-\infty}^{+\infty} \phi^\tau(t-s) ds = (M + 2\mathcal{K}(t)) \|\psi_\eta\|_{W^1_\infty(\mathbb{R}^d)}$$

6. By the definition of Q^τ we have

$$\begin{aligned} |\partial_t Q_\eta^\tau(t;\boldsymbol{x},\boldsymbol{z})| &= \left| \int_{-\infty}^{+\infty} Q_\eta(s;\boldsymbol{x},\boldsymbol{z}) \frac{d}{dt} \phi^\tau(t-s) ds \right| \leq \int_{-\infty}^{+\infty} |Q_\eta(s;\boldsymbol{x},\boldsymbol{z})| |D_t \phi^\tau(t-s)| ds \\ &\leq M \|\psi_\eta\|_{W^0_\infty(\mathbb{R}^d)} \int_{-\infty}^{+\infty} |D_t \phi^\tau(t-s)| ds \leq M \|\psi_\eta\|_{W^0_\infty(\mathbb{R}^d)} \|\phi^\tau\|_{W^1_1(\mathbb{R}^d)} \end{aligned}$$

7. Rewrite equation (3.23) applied to $\boldsymbol{f}^\tau$ and Q^τ in the form

$$i\boldsymbol{z}\cdot\boldsymbol{f}^\tau(t;\boldsymbol{x},\boldsymbol{z}) = i\,\mathrm{div}_{\boldsymbol{x}}\,\nabla_{\boldsymbol{z}}Q^\tau_\eta(t;\boldsymbol{x},\boldsymbol{z}) - \partial_t Q^\tau_\eta(t;\boldsymbol{x},\boldsymbol{z})$$

and use the triangle inequality

$$|\boldsymbol{z}\cdot\boldsymbol{f}^\tau(t;\boldsymbol{x},\boldsymbol{z})| \le |\,\mathrm{div}_{\boldsymbol{x}}\,\nabla_{\boldsymbol{z}}Q^\tau_\eta(t;\boldsymbol{x},\boldsymbol{z})| + |\partial_t Q^\tau_\eta(t;\boldsymbol{x},\boldsymbol{z})|$$

Next, apply statements 5 and 6 of this theorem:

$$|\boldsymbol{z}\cdot\boldsymbol{f}^\tau(t;\boldsymbol{x},\boldsymbol{z})| \le (M+2\mathcal{K}(t))\|\psi_\eta\|_{W^1_\infty(\mathbb{R}^d)} + M\|\psi_\eta\|_{W^0_\infty(\mathbb{R}^d)}\|\phi^\tau\|_{W^1_1(\mathbb{R}^d)}$$

□

CHAPTER FOUR

APPROXIMATE CLOSURE

4.6 Forcing term

Recall that

$$\boldsymbol{f}_\eta(t;\boldsymbol{x},\boldsymbol{z}) = \frac{1}{N}\sum_{j=1}^{N}\left\{-\frac{1}{\varepsilon}\sum_{k=1}^{N}\nabla U\left(\frac{\boldsymbol{q}_j(t)-\boldsymbol{q}_k(t)}{\varepsilon}\right)\right\} e^{i\boldsymbol{v}_j(t)\cdot\boldsymbol{z}}\psi_\eta(\boldsymbol{x}-\boldsymbol{q}_j(t))$$

Denote

$$\boldsymbol{\kappa}_{j,k}(t) = \frac{\boldsymbol{q}_j(t)-\boldsymbol{q}_k(t)}{\varepsilon}$$

Using the notation rewrite the formula for $\boldsymbol{f}_\eta(t;\boldsymbol{x},\boldsymbol{z})$ in the form

$$\begin{aligned}
\boldsymbol{f}_\eta(t;\boldsymbol{x},\boldsymbol{z}) &= \frac{1}{N}\sum_{j=1}^{N}\left\{-\frac{1}{\varepsilon}\sum_{k=1}^{N}\nabla U(\boldsymbol{\kappa}_{j,k}(t))\right\} e^{i\boldsymbol{v}_j(t)\cdot\boldsymbol{z}}\psi_\eta(\boldsymbol{x}-\boldsymbol{q}_j(t)) \\
&= -\frac{1}{2}\frac{1}{N}\sum_{k,j=1}^{N}\frac{1}{\varepsilon}\nabla U(\boldsymbol{\kappa}_{j,k}(t))\{e^{i\boldsymbol{v}_j(t)\cdot\boldsymbol{z}}\psi_\eta(\boldsymbol{x}-\boldsymbol{q}_j(t)) - e^{i\boldsymbol{v}_k(t)\cdot\boldsymbol{z}}\psi_\eta(\boldsymbol{x}-\boldsymbol{q}_k(t))\} \\
&= -\frac{1}{2}\frac{1}{N}\sum_{k,j=1}^{N}\nabla U(\boldsymbol{\kappa}_{j,k}(t))\frac{e^{i\boldsymbol{v}_j(t)\cdot\boldsymbol{z}}\psi_\eta(\boldsymbol{x}-\boldsymbol{q}_j(t)) - e^{i\boldsymbol{v}_k(t)\cdot\boldsymbol{z}}\psi_\eta(\boldsymbol{x}-\boldsymbol{q}_k(t))}{\varepsilon}
\end{aligned}$$

Next, consider function $g:\mathbb{R}^{2d}\to\mathbb{R}$ defined by

$$g(\boldsymbol{w}) = e^{i\boldsymbol{w}_1\cdot\boldsymbol{z}}\psi_\eta(\boldsymbol{x}-\boldsymbol{w}_2) \tag{4.26}$$

where $\boldsymbol{w}=(\boldsymbol{w}_1,\boldsymbol{w}_2)\in\mathbb{R}^{2d}$. Using the Fundamental Theorem of Calculus we can write the integral representation of the difference:

$$g(\boldsymbol{w}_2)-g(\boldsymbol{w}_1) = (\boldsymbol{w}_2-\boldsymbol{w}_1)\cdot\int_0^1\nabla g(\boldsymbol{w}_1+s(\boldsymbol{w}_2-\boldsymbol{w}_1))ds$$

Using the values

$$\boldsymbol{w}_2 = (\boldsymbol{v}_j(t),\boldsymbol{q}_j(t)), \qquad \boldsymbol{w}_1 = (\boldsymbol{v}_k(t),\boldsymbol{q}_k(t))$$

in the formula above, write

$$\frac{g((\boldsymbol{v}_j(t),\boldsymbol{q}_j(t))) - g((\boldsymbol{v}_k(t),\boldsymbol{q}_k(t)))}{\varepsilon} = \int_0^1 \{\dot{\boldsymbol{\kappa}}_{j,k}(t)\cdot\nabla_1 g(A) + \boldsymbol{\kappa}_{j,k}(t)\cdot\nabla_2 g(A)\}ds \tag{4.27}$$

where expresion A is defined by

$$\begin{aligned} A &= (\boldsymbol{v}_k(t) + (\boldsymbol{v}_j(t) - \boldsymbol{v}_k(t))s, \boldsymbol{q}_k(t) + (\boldsymbol{q}_j(t) - \boldsymbol{q}_k(t))s) \\ &= (\boldsymbol{v}_k(t) + \varepsilon\dot{\boldsymbol{\kappa}}_{j,k}(t)s, \boldsymbol{q}_k(t) + \varepsilon\boldsymbol{\kappa}_{j,k}(t)s) \end{aligned}$$

Further, using (4.26) we compute $\nabla_1 g$ and $\nabla_2 g$:

$$\nabla_1 g(\boldsymbol{w}) = ize^{i\boldsymbol{w}_1\cdot\boldsymbol{z}}\psi_\eta(\boldsymbol{x}-\boldsymbol{w}_2), \qquad \nabla_2 g(\boldsymbol{w}) = -e^{i\boldsymbol{w}_1\cdot\boldsymbol{z}}\nabla\psi_\eta(\boldsymbol{x}-\boldsymbol{w}_2)$$

Define

$$I^\varepsilon_{j,k}(t;\boldsymbol{x},\boldsymbol{z}) = \int_0^1 e^{i\varepsilon\dot{\boldsymbol{\kappa}}_{j,k}(t)\cdot\boldsymbol{z}s}\psi_\eta(\boldsymbol{x}-\boldsymbol{q}_k-\varepsilon\boldsymbol{\kappa}_{j,k}(t)s)ds$$

Having computed $\nabla_1 g$ and $\nabla_2 g$, simplify the right hand side of (4.27):

$$\begin{aligned} &\int_0^1 \{\dot{\boldsymbol{\kappa}}_{j,k}(t)\cdot\nabla_1 g(A) + \boldsymbol{\kappa}_{j,k}(t)\cdot\nabla_2 g(A)\}ds \\ &\qquad = ie^{i\boldsymbol{v}_k\cdot\boldsymbol{z}}\dot{\boldsymbol{\kappa}}_{j,k}(t)\cdot z I^\varepsilon_{j,k}(t;\boldsymbol{x},\boldsymbol{z}) - e^{i\boldsymbol{v}_k\cdot\boldsymbol{z}}\boldsymbol{\kappa}_{j,k}(t)\cdot\nabla_{\boldsymbol{x}} I^\varepsilon_{j,k}(t;\boldsymbol{x},\boldsymbol{z}) \end{aligned}$$

Therefore,

$$\begin{aligned} \boldsymbol{f}_\eta(t;\boldsymbol{x},\boldsymbol{z}) &= -\frac{1}{2}\frac{1}{N}\sum_{k,j=1}^N \nabla U(\boldsymbol{\kappa}_{j,k}(t)) ie^{i\boldsymbol{v}_k\cdot\boldsymbol{z}}\{\dot{\boldsymbol{\kappa}}_{j,k}(t)\cdot z\} I^\varepsilon_{j,k}(t;\boldsymbol{x},\boldsymbol{z}) \\ &\quad + \frac{1}{2}\frac{1}{N}\sum_{k,j=1}^N \nabla U(\boldsymbol{\kappa}_{j,k}(t)) e^{i\boldsymbol{v}_k\cdot\boldsymbol{z}}\left\{\boldsymbol{\kappa}_{j,k}(t)\cdot\nabla_{\boldsymbol{x}} I^\varepsilon_{j,k}(t;\boldsymbol{x},\boldsymbol{z})\right\} \end{aligned} \tag{4.28}$$

Lemma 1. *The quantities $I^\varepsilon_{j,k}(t;\boldsymbol{x},\boldsymbol{z})$ and $\nabla_{\boldsymbol{x}} I^\varepsilon_{j,k}(t;\boldsymbol{x},\boldsymbol{z})$ can be written in the form*

$$I^\varepsilon_{j,k}(t;\boldsymbol{x},\boldsymbol{z}) = \varphi(i\varepsilon\dot{\boldsymbol{\kappa}}_{j,k}(t)\cdot\boldsymbol{z})\psi_\eta(\boldsymbol{x}-\boldsymbol{q}_k) + R_1$$

and

$$\nabla_{\boldsymbol{x}} I^{\varepsilon}_{j,k}(t;\boldsymbol{x},\boldsymbol{z}) = \varphi(i\varepsilon\dot{\boldsymbol{\kappa}}_{j,k}(t)\cdot\boldsymbol{z})\nabla_{\boldsymbol{x}}\psi_\eta(\boldsymbol{x}-\boldsymbol{q}_k) + \boldsymbol{R}_2$$

where $\varphi(x)$ is the continuous function defined by

$$\varphi(x) = \int_0^1 e^{xs}ds = \begin{cases} \dfrac{e^x-1}{x} & x \neq 0 \\ 1 & x = 0 \end{cases}$$

and the terms R_1 and $\boldsymbol{R}_2$ are bounded

$$|R_1| \leq \varepsilon\|\boldsymbol{\kappa}_{j,k}(t)\|_2\|\psi_\eta\|_{W^1_\infty(\mathbb{R}^d)} \qquad \|\boldsymbol{R}_2\|_2 \leq \varepsilon\|\boldsymbol{\kappa}_{j,k}(t)\|_2\|\psi_\eta\|_{W^2_\infty(\mathbb{R}^d)}$$

Proof. Recall the definition of $I^{\varepsilon}_{j,k}(t;\boldsymbol{z},\boldsymbol{z})$

$$I^{\varepsilon}_{j,k}(t;\boldsymbol{x},\boldsymbol{z}) = \int_0^1 e^{i\varepsilon\dot{\boldsymbol{\kappa}}_{j,k}(t)\cdot\boldsymbol{z}s}\psi_\eta(\boldsymbol{x}-\boldsymbol{q}_k-\varepsilon\boldsymbol{\kappa}_{j,k}(t)s)ds$$

Consider

$$\begin{aligned} R_1 &= I^{\varepsilon}_{j,k}(t;\boldsymbol{x},\boldsymbol{z}) - \psi_\eta(\boldsymbol{x}-\boldsymbol{q}_k)\int_0^1 e^{i\varepsilon\dot{\boldsymbol{\kappa}}_{j,k}(t)\cdot\boldsymbol{z}s}ds \\ &= \int_0^1 e^{i\varepsilon\dot{\boldsymbol{\kappa}}_{j,k}(t)\cdot\boldsymbol{z}s}(\psi_\eta(\boldsymbol{x}-\boldsymbol{q}_k-\varepsilon\boldsymbol{\kappa}_{j,k}(t)s) - \psi_\eta(\boldsymbol{x}-\boldsymbol{q}_k))ds \\ &= -\int_0^1 e^{i\varepsilon\dot{\boldsymbol{\kappa}}_{j,k}(t)\cdot\boldsymbol{z}s}\left\{\varepsilon\boldsymbol{\kappa}_{j,k}(t)s\cdot\int_0^1\nabla_{\boldsymbol{x}}\psi_\eta(\boldsymbol{x}-\boldsymbol{q}_k-\sigma\varepsilon\boldsymbol{\kappa}_{j,k}(t)s)d\sigma\right\}ds \end{aligned}$$

Therefore,

$$|R_1| \leq \varepsilon\|\boldsymbol{\kappa}_{j,k}(t)\|_2\|\psi_\eta\|_{W^1_\infty(\mathbb{R}^d)}$$

Next, consider

$$\begin{aligned} \boldsymbol{R}_2 &= \nabla_{\boldsymbol{x}} I^{\varepsilon}_{j,k}(t;\boldsymbol{x},\boldsymbol{z}) - \nabla_{\boldsymbol{x}}\psi_\eta(\boldsymbol{x}-\boldsymbol{q}_k)\int_0^1 e^{i\varepsilon\dot{\boldsymbol{\kappa}}_{j,k}(t)\cdot\boldsymbol{z}s}ds \\ &= \int_0^1 e^{i\varepsilon\dot{\boldsymbol{\kappa}}_{j,k}(t)\cdot\boldsymbol{z}s}(\nabla_{\boldsymbol{x}}\psi_\eta(\boldsymbol{x}-\boldsymbol{q}_k-\varepsilon\boldsymbol{\kappa}_{j,k}(t)s) - \nabla_{\boldsymbol{x}}\psi_\eta(\boldsymbol{x}-\boldsymbol{q}_k))ds \\ &= -\int_0^1 e^{i\varepsilon\dot{\boldsymbol{\kappa}}_{j,k}(t)\cdot\boldsymbol{z}s}\left\{\int_0^1\nabla_{\boldsymbol{x}}\nabla_{\boldsymbol{x}}\psi_\eta(\boldsymbol{x}-\boldsymbol{q}_k-\sigma\varepsilon\boldsymbol{\kappa}_{j,k}(t)s)d\sigma\right\}\varepsilon\boldsymbol{\kappa}_{j,k}(t)sds \end{aligned}$$

Hence,

$$\|\boldsymbol{R}_2\|_2 \leq \varepsilon \|\boldsymbol{\kappa}_{j,k}(t)\|_2 \|\psi_\eta\|_{W^2_\infty(\mathbb{R}^d)}$$

□

4.7 Restrictions on dynamics

Assume that any two interacting particles have similar velocities:

$$\|\dot{\boldsymbol{\kappa}}_{j,k}(t)\|_2 \leq C_{\boldsymbol{v}} \qquad \text{if } \nabla U(\boldsymbol{\kappa}_{j,k}(t)) \neq 0 \tag{4.29}$$

for some fixed constant C independent of N. Since the the potential function U has a bounded support, for any two interracting particles we also have

$$\|\boldsymbol{\kappa}_{j,k}(t)\|_2 \leq C_{\boldsymbol{\kappa}} \qquad \text{if } \nabla U(\boldsymbol{\kappa}_{j,k}(t)) \neq 0 \tag{4.30}$$

Assume also that for all j, k, t, and N we have

$$\|\boldsymbol{\kappa}_{j,k}(t)\|_2 \geq c_{\boldsymbol{\kappa}}$$

This assumption implies that for all j, k, t, and N we have

$$\|\nabla U(\boldsymbol{\kappa}_{j,k}(t))\|_2 \leq C_{\boldsymbol{f}} \tag{4.31}$$

Define

$$\begin{aligned}
\tilde{\boldsymbol{f}}_\eta(t;\boldsymbol{x},\boldsymbol{z}) &= -\frac{1}{2}\frac{1}{N}\sum_{k,j=1}^{N} \nabla U(\boldsymbol{\kappa}_{j,k}(t)) i e^{i\boldsymbol{v}_k\cdot\boldsymbol{z}} \{\dot{\boldsymbol{\kappa}}_{j,k}(t)\cdot z\}\psi_\eta(\boldsymbol{x}-\boldsymbol{q}_k) \\
&\quad + \frac{1}{2}\frac{1}{N}\sum_{k,j=1}^{N} \nabla U(\boldsymbol{\kappa}_{j,k}(t)) e^{i\boldsymbol{v}_k\cdot\boldsymbol{z}} \{\boldsymbol{\kappa}_{j,k}(t)\cdot\nabla\psi_\eta(\boldsymbol{x}-\boldsymbol{q}_k)\}
\end{aligned}$$

The following lemma shows that the quantity $\tilde{\boldsymbol{f}}_\eta(t;\boldsymbol{x},\boldsymbol{z})$ gives an approximation to $\boldsymbol{f}_\eta(t;\boldsymbol{x},\boldsymbol{z})$ if the assumptions hold.

Lemma 2. *Conditions (4.29), (4.30), (4.28), and (4.31) imply*

$$\|\boldsymbol{f}_\eta(t;\boldsymbol{x},\boldsymbol{z}) - \tilde{\boldsymbol{f}}_\eta(t;\boldsymbol{x},\boldsymbol{z})\| \le C_a\varepsilon$$

for some constant C_a independent of N.

Proof. Notice that condition (4.31) and the fact that U has bounded support implies that the number of neighbors of any particle is bounded by a number independent of N. Indeed, let $\operatorname{supp} U \subset B_r(0)$, where $B_r(0)$ is a ball centered at 0 of radius r. Then $\operatorname{supp} U(\boldsymbol{x}/\varepsilon) \subset \varepsilon B_r(0)$. For a fixed number j we would like to count particles for which

$$U\left(\frac{\boldsymbol{q}_j(t) - \boldsymbol{q}_k(t)}{\varepsilon}\right) \neq 0 \qquad \text{or} \qquad \|\boldsymbol{q}_j(t) - \boldsymbol{q}_k(t)\|_2 \le \varepsilon r$$

Since the minimum distance between particles is $\varepsilon c_{\boldsymbol{\kappa}}$, the balls $B_{\varepsilon c_{\boldsymbol{\kappa}}/2}(\boldsymbol{q}_j(t))$ do not intersect. Next,

$$\text{Volume}(B_r(0)) = r^d B_1(0), \qquad \text{Volume}(B_{\varepsilon c_{\boldsymbol{\kappa}}/2}(\boldsymbol{q}_j(t))) = \left(\frac{\varepsilon c_{\boldsymbol{\kappa}}}{2}\right)^d B_1(0)$$

Hence, the number of interacting neighbors is bounded by the quantity

$$\frac{\text{Volume}(B_r(0))}{\text{Volume}(B_{\varepsilon c_{\boldsymbol{\kappa}}/2}(\boldsymbol{q}_j(t)))} = \frac{r^d 2^d}{\varepsilon^d c_{\boldsymbol{\kappa}}^d} = M$$

which is independent of N.

Next, consider the difference $\tilde{\boldsymbol{f}}_\eta(t;\boldsymbol{x},\boldsymbol{z}) - \boldsymbol{f}_\eta(t;\boldsymbol{x},\boldsymbol{z})$:

$$\begin{aligned}\tilde{\boldsymbol{f}}_\eta(t;\boldsymbol{x},\boldsymbol{z}) - \boldsymbol{f}_\eta(t;\boldsymbol{x},\boldsymbol{z}) &= -\frac{1}{2}\frac{1}{N}\sum_{k,j=1}^{N} \nabla U(\boldsymbol{\kappa}_{j,k}(t)) i e^{i\boldsymbol{v}_k\cdot\boldsymbol{z}}\{\dot{\boldsymbol{\kappa}}_{j,k}(t)\cdot z\}(I^\varepsilon_{j,k}(t;\boldsymbol{x},\boldsymbol{z}) - \psi_\eta(\boldsymbol{x}-\boldsymbol{q}_k)) \\ &\quad + \frac{1}{2}\frac{1}{N}\sum_{k,j=1}^{N} \nabla U(\boldsymbol{\kappa}_{j,k}(t)) e^{i\boldsymbol{v}_k\cdot\boldsymbol{z}}\left\{\boldsymbol{\kappa}_{j,k}(t)\cdot(\nabla_{\boldsymbol{x}} I^\varepsilon_{j,k}(t;\boldsymbol{x},\boldsymbol{z}) - \nabla\psi_\eta(\boldsymbol{x}-\boldsymbol{q}_k))\right\}\end{aligned}$$

Using Lemma 1 we find

$$\|\tilde{\boldsymbol{f}}_\eta(t;\boldsymbol{x},\boldsymbol{z}) - \boldsymbol{f}_\eta(t;\boldsymbol{x},\boldsymbol{z})\|_2 \le C_a\varepsilon$$

where C_a is a constant independent of N. □

Further, rearranging summation in (4.32), expression for $\boldsymbol{z}\cdot\tilde{\boldsymbol{f}}_\eta(t;\boldsymbol{x},\boldsymbol{z})$ can be rewritten as

$$\begin{aligned}\boldsymbol{z}\cdot\tilde{\boldsymbol{f}}_\eta(t;\boldsymbol{x},\boldsymbol{z}) &= -i\frac{1}{2}\frac{1}{N}\sum_{k=1}^{N}\left\{\sum_{j=1}^{N}(\boldsymbol{z}\cdot\nabla U(\boldsymbol{\kappa}_{j,k}(t)))(\dot{\boldsymbol{\kappa}}_{j,k}(t)\cdot\boldsymbol{z})\right\}e^{i\boldsymbol{v}_k\cdot\boldsymbol{z}}\psi_\eta(\boldsymbol{x}-\boldsymbol{q}_k) \\ &\quad +\boldsymbol{z}\cdot\mathrm{div}_{\boldsymbol{x}}\left\{\frac{1}{2}\frac{1}{N}\sum_{k=1}^{N}\left\{\sum_{k=1}^{N}\nabla U(\boldsymbol{\kappa}_{j,k}(t))\otimes\boldsymbol{\kappa}_{j,k}(t)\right\}e^{i\boldsymbol{v}_k\cdot\boldsymbol{z}}\psi_\eta(\boldsymbol{x}-\boldsymbol{q}_k)\right\}\end{aligned} \tag{4.32}$$

4.8 Approximate closure

It appears that function $Q_\eta(t;\boldsymbol{x},\boldsymbol{z})$ has no information about distances between interacting particles. Indeed, consider the examples on Figure 4.4. The periodic structures on the figure have different densities, however, the distances between interacting particles are the same. If we assume that the velocities of all particles are 0, then $Q_\eta(t;\boldsymbol{x},\boldsymbol{z})=\rho_\eta(t;\boldsymbol{x})$, and we can claim that different values of $Q_\eta(t;\boldsymbol{x},\boldsymbol{z})$ correspond to equal distances between interacting particles. It shows that the information about the distances of interacting particles cannot be found from $Q_\eta(t;\boldsymbol{x},\boldsymbol{z})$ in the general case.

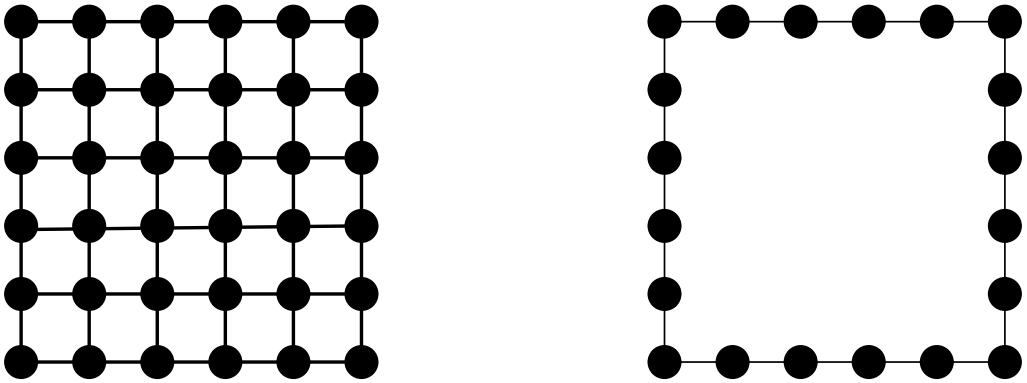

(a) Rectangular lattice (b) Rectangle

Figure 4.4: Interacting structures

Although we can not find a representation of $\boldsymbol{f}_\eta(t;\boldsymbol{x},\boldsymbol{z})$ in terms of $Q_\eta(t;\boldsymbol{x},\boldsymbol{z})$ in the general case, we can use some approximations for particular scenarios.

Assume that in the vicinity of every point $\boldsymbol{x}\in\Omega$ the distance between interacting particles is inversely proportional to $\rho_\eta(t;\boldsymbol{x})^{\frac{1}{d}}$. Indeed, the more particles we have in a d-dimensional region, the less distance between every particle should be in that region. Also, assume that the material

is isotropic. Then approximate

$$\sum_{k=1}^{N} \nabla U(\boldsymbol{\kappa}_{j,k}(t)) \otimes \boldsymbol{\kappa}_{j,k}(t) \approx \frac{\alpha_1}{\rho_\eta(t;\boldsymbol{x})^{\frac{1}{d}}} u'\left(\frac{\beta_1}{\rho_\eta(t;\boldsymbol{x})^{\frac{1}{d}}}\right) I$$

for some fixed constants α_1 and β_1. To approximate $\dot{\boldsymbol{\kappa}}_{j,k}$ we will use the quantity

$$\frac{\alpha_2}{\rho_\eta(t;\boldsymbol{x})^{\frac{1}{d}}} \operatorname{div}_{\boldsymbol{x}}\left(\frac{\boldsymbol{p}_\eta(t;\boldsymbol{x})}{\rho_\eta(t;\boldsymbol{x})}\right)$$

which represents the relative flow of particles through the boundary of an infinitesimal region, hence correlates with the rate of change of the average distance between particles. Assuming isotropy, we approximate

$$\sum_{k=1}^{N} \nabla U(\boldsymbol{\kappa}_{j,k}(t)) \otimes \dot{\boldsymbol{\kappa}}_{j,k}(t) \approx \frac{\alpha_2}{\rho_\eta(t;\boldsymbol{x})^{\frac{1}{d}}} \operatorname{div}_{\boldsymbol{x}}\left(\frac{\boldsymbol{p}_\eta(t;\boldsymbol{x})}{\rho_\eta(t;\boldsymbol{x})}\right) u'\left(\frac{\beta_2}{\rho_\eta(t;\boldsymbol{x})^{\frac{1}{d}}}\right) I$$

for some fixed constants α_2 and β_2. Using these approximations our formula (4.32) becomes

$$\begin{aligned} \boldsymbol{z} \cdot \tilde{\boldsymbol{f}}_\eta(t;\boldsymbol{x},\boldsymbol{z}) \quad \approx \quad & -\frac{i\alpha_2}{2} \operatorname{div}_{\boldsymbol{x}}\left(\frac{\boldsymbol{p}_\eta(t;\boldsymbol{x})}{\rho_\eta(t;\boldsymbol{x})}\right) \frac{\boldsymbol{z}\cdot\boldsymbol{z}}{\rho_\eta(t;\boldsymbol{x})^{\frac{1}{d}}} u'\left(\frac{\beta_2}{\rho_\eta(t;\boldsymbol{x})^{\frac{1}{d}}}\right) Q_\eta(t;\boldsymbol{x},\boldsymbol{z}) \\ & + \operatorname{div}_{\boldsymbol{x}}\left\{\frac{\alpha_1}{2} u'\left(\frac{\beta_1}{\rho_\eta(t;\boldsymbol{x})^{\frac{1}{d}}}\right) \boldsymbol{z} \frac{Q_\eta(t;\boldsymbol{x},\boldsymbol{z})}{\rho_\eta(t;\boldsymbol{x})^{\frac{1}{d}}}\right\} \end{aligned} \tag{4.33}$$

where, as before,

$$\rho_\eta(t;\boldsymbol{x}) = Q_\eta(t;\boldsymbol{x},0), \qquad \boldsymbol{p}_\eta(t;\boldsymbol{x}) = -i\nabla_{\boldsymbol{z}} Q(t;\boldsymbol{x},0)$$

Formula (4.33) is a closure that works at least for the case when the particle system is a discretization of a PDE (details are given in section 5.12). For all other particle systems this closure may be used as an approximation of $\boldsymbol{f}_\eta(t;\boldsymbol{x},\boldsymbol{z})$. The constants $\alpha_1, \alpha_2, \beta_1, \beta_2$ can be obtained experimentally, they depend on the dynamics of the system.

4.9 Algorithm

In this section we present an algorithm for computing function $Q_\eta(t;\boldsymbol{x},\boldsymbol{z})$ using approximation (4.33). For the sake of argument, in this section we consider the case $d = 1$. However, everything

can be generalized to the case of higher dimensions.

Suppose we are given a potential $U^{(\text{ext})}(\boldsymbol{x})$ that generates an external force on a particle j by the law

$$\boldsymbol{f}_j^{(\text{ext})} = -\frac{1}{N}\nabla U^{(\text{ext})}(\boldsymbol{q}_j).$$

This law can model gravitational forces, electrostatic forces, and many others where the force is proportional to the mass of particles (for example if we assume that the amount of charge is proportional to the mass of particles, then electrostatic forces can be described by the model). Assume that $\nabla U^{(\text{ext})}(\boldsymbol{x})$ is a smooth function.

Suppose that due to the external forces the particles cannot leave some region inside Ω, so there are no particles within radius η from the boundary of Ω:

$$\boldsymbol{q}_j \notin \bigcup_{\boldsymbol{x}\in\partial\Omega} B_\eta(\boldsymbol{x})$$

Pick a smooth function ψ such that $\operatorname{supp}\psi \subset (-1,1)$. Then $\operatorname{supp}\psi_\eta \subset (-\eta,\eta)$ and by the definition of $Q_\eta(t;\boldsymbol{x},\boldsymbol{z})$ we have

$$Q_\eta(t;\boldsymbol{x},\boldsymbol{z}) = 0 \qquad \text{for all } \boldsymbol{x}\in\partial\Omega \text{ and } \boldsymbol{z}\in\mathbb{R}^d \tag{4.34}$$

Next, because of the external forces the forcing term $\boldsymbol{f}_\eta(t;\boldsymbol{x},\boldsymbol{z})$ takes the form

$$\begin{aligned}\boldsymbol{f}_\eta(t;\boldsymbol{x},\boldsymbol{z}) \;=\; & \frac{1}{N}\sum_{j=1}^{N}\left\{-\frac{1}{\varepsilon}\sum_{k=1}^{N}\nabla U\left(\frac{\boldsymbol{q}_j(t)-\boldsymbol{q}_k(t)}{\varepsilon}\right)\right\} e^{i\boldsymbol{v}_j(t)\cdot\boldsymbol{z}}\psi_\eta(\boldsymbol{x}-\boldsymbol{q}_j(t)) \\ & -\frac{1}{N}\sum_{j=1}^{N}\nabla U^{(\text{ext})}(\boldsymbol{q}_j)e^{i\boldsymbol{v}_j(t)\cdot\boldsymbol{z}}\psi_\eta(\boldsymbol{x}-\boldsymbol{q}_j(t))\end{aligned} \tag{4.35}$$

Observe that since $\operatorname{supp}\psi_\eta(\boldsymbol{x}) \subset B_\eta(0)$, in (4.35) the sums are over the particles that are in the ball $B_\eta(\boldsymbol{x})$. Using the smoothness of U for $\|\boldsymbol{q}_j-\boldsymbol{x}\|_2 \le \eta$ rewrite

$$\nabla U^{(\text{ext})}(\boldsymbol{q}_j) = \nabla U^{(\text{ext})}(\boldsymbol{x}) + \boldsymbol{R}_1$$

where

$$\|\boldsymbol{R}_1\|_2 \leq \eta C_U$$

Hence,

$$\frac{1}{N}\sum_{j=1}^{N} \nabla U^{(\text{ext})}(\boldsymbol{q}_j) e^{i\boldsymbol{v}_j(t)\cdot\boldsymbol{z}} \psi_\eta(\boldsymbol{x}-\boldsymbol{q}_j(t)) = \frac{1}{M}\nabla U^{(\text{ext})}(\boldsymbol{x}) Q_\eta(t;\boldsymbol{x},\boldsymbol{z}) + \boldsymbol{R}_2 \tag{4.36}$$

where

$$\|\boldsymbol{R}_2\|_2 \leq \eta C_U \rho_\eta(t;\boldsymbol{x})$$

Using (4.36) approximate $\boldsymbol{z}\cdot\boldsymbol{f}_\eta(t;\boldsymbol{x},\boldsymbol{z})$:

$$\begin{aligned}
\boldsymbol{z}\cdot\boldsymbol{f}_\eta(t;\boldsymbol{x},\boldsymbol{z}) \;\approx\; & -\frac{i\alpha_2}{2}\,\mathrm{div}_{\boldsymbol{x}}\left(\frac{\boldsymbol{p}_\eta(t;\boldsymbol{x})}{\rho_\eta(t;\boldsymbol{x})}\right)\frac{\boldsymbol{z}\cdot\boldsymbol{z}}{\rho_\eta(t;\boldsymbol{x})^{\frac{1}{d}}}u'\left(\frac{\beta_2}{\rho_\eta(t;\boldsymbol{x})^{\frac{1}{d}}}\right)Q_\eta(t;\boldsymbol{x},\boldsymbol{z}) \\
& + \mathrm{div}_{\boldsymbol{x}}\left\{\frac{\alpha_1}{2}u'\left(\frac{\beta_1}{\rho_\eta(t;\boldsymbol{x})^{\frac{1}{d}}}\right)\boldsymbol{z}\frac{Q_\eta(t;\boldsymbol{x},\boldsymbol{z})}{\rho_\eta(t;\boldsymbol{x})^{\frac{1}{d}}}\right\} \\
& -\boldsymbol{z}\cdot\nabla U^{(\text{ext})}(\boldsymbol{x})\frac{Q_\eta(t;\boldsymbol{x},\boldsymbol{z})}{M}
\end{aligned} \tag{4.37}$$

Using approximation (4.37) we can define the algorithm for numerical computation of $Q_\eta(t;\boldsymbol{x},\boldsymbol{z})$. Since we have no boundary conditions in the $\boldsymbol{z}$ space, we can either use one-sided derivative schemes on the boundary of $\boldsymbol{z}$ region or drop the boundary nodes on every time step (see Figure 4.5). The later idea is based on the fact that the standard quantities are obtained from Q_η at $\boldsymbol{z}=0$.

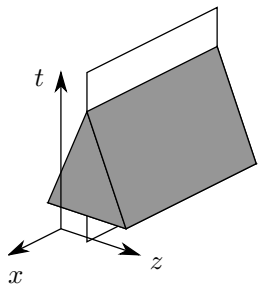

Figure 4.5: Triangular scheme

CHAPTER FIVE

EXAMPLES

5.10 Ideal gas

The easiest example is the ideal gas. It can be modeled by the equations (3.23) and (3.25), where the potential function U is taken to be 0 (no interparticle forces). Hence, we get $\boldsymbol{f} = 0$ in (3.23) and

$$\partial_t Q_\eta(t; \boldsymbol{x}, \boldsymbol{z}) = i \operatorname{div}_{\boldsymbol{x}} \nabla_{\boldsymbol{z}} Q_\eta(t; \boldsymbol{x}, \boldsymbol{z}) \tag{5.38}$$

Suppose, we are given an initial condition

$$Q_\eta(0; \boldsymbol{x}, \boldsymbol{z}) = Q_0(\boldsymbol{x}, \boldsymbol{z}) \tag{5.39}$$

To find solution $Q_\eta(t; \boldsymbol{x}, \boldsymbol{z})$ of the initial value problem (5.38, 5.39) we will apply Fourier transform to the both sides of (5.38) and use the fact that the derivatives with respect to $\boldsymbol{x}$ turn into multiplication by $i\boldsymbol{\xi}$:

$$\partial_t \mathcal{F}_{\boldsymbol{x}}[Q_\eta(t; \boldsymbol{x}, \boldsymbol{z})](\boldsymbol{\xi}) = -\boldsymbol{\xi} \cdot \nabla_{\boldsymbol{z}} \mathcal{F}_{\boldsymbol{x}}[Q_\eta(t; \boldsymbol{x}, \boldsymbol{z})](\boldsymbol{\xi})$$

Since function $Q_\eta(t; \boldsymbol{x}, \boldsymbol{z})$ has bounded support with respect to $\boldsymbol{x}$ and is smooth by definition (3.22), the Fourier transform exists. Next, solve the obtained equation using the method of characteristics:

$$\mathcal{F}_{\boldsymbol{x}}[Q_\eta(t; \boldsymbol{x}, \boldsymbol{z})](\boldsymbol{\xi}) = \mathcal{F}_{\boldsymbol{x}}[Q_0(\boldsymbol{x}, \boldsymbol{z} - t\boldsymbol{\xi})](\boldsymbol{\xi})$$

Finally, apply the inverse Fourier transform

$$Q_\eta(t; \boldsymbol{x}, \boldsymbol{z}) = \mathcal{F}^{-1}_{\boldsymbol{\xi}}[\mathcal{F}_{\boldsymbol{x}}[Q_0(\boldsymbol{\xi}, \boldsymbol{z} - t\boldsymbol{\xi})](\boldsymbol{\xi})](\boldsymbol{x})$$

Therefore, for the ideal gas an explicit formula can be derived for the evolution of the function $Q_\eta(t; \boldsymbol{x}, \boldsymbol{z})$.

5.11 Lennard-Jones like potential

In this example we use a potential function that is qualitatively close to the Leonard-Jones potential. This function is better for computational purposes because of its moderate slope. (We have to perform more operations to evaluate this potential, but we can make wider time steps).

Consider a one dimensional problem governed by the potential

$$u(x) = \begin{cases} -1600 + 5568x + \dfrac{192}{x} - 10560x^2 + 11840x^3 - 7872x^4 + 2880x^5 - 448x^6 & x > 0 \\ 0 & x \leq 0 \end{cases}$$

with the conditions

- at $t = 0$ $\boldsymbol{q}_j < \boldsymbol{q}_{i+1}$ for all $0 < i < N$
- $\boldsymbol{q}_1 = 0$ and $\boldsymbol{q}_N = 1$ for all t

The graph of this potential and the graph of the corresponding force are given on figure 5.6. The particles of the system will be always ordered, since $u(x) \to \infty$ as $x \to 0^+$. That is

$$\boldsymbol{q}_j < \boldsymbol{q}_j \quad \text{if} \quad i < j$$

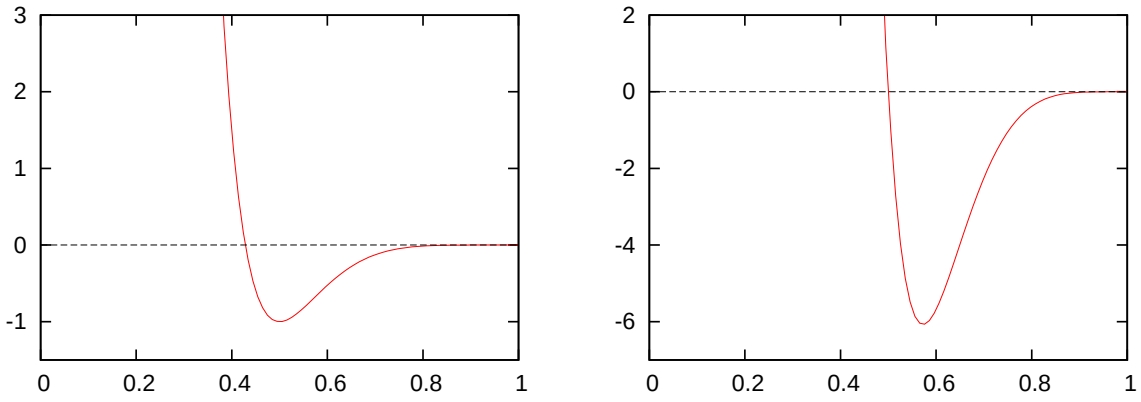

(a) Potential (b) Force

Figure 5.6: Particle interaction

In this experiment we numerically solved the system of differential equations (1.6). Using the solution, we computed the quantities $Q_\eta^\tau(t; \boldsymbol{x}, \boldsymbol{z})$ and $\boldsymbol{f}_\eta^\tau(t; \boldsymbol{x}, \boldsymbol{z})$ and checked the equations of the

approximate closure given in (4.33). The results of the numerical experiment are graphed on Figure 5.7.

Although the approximate closure was derived for the quantities without time averages, in this experiment we use the time averaged quantities in all formulas. This decision is based on the practical considerations: Without time averaging the quantity $\boldsymbol{f}_\eta(t;\boldsymbol{x},\boldsymbol{z})$ can be unbounded.

During the experiment it was possible to find constants $\alpha_1, \alpha_2, \beta_1, \beta_2$ such that the approximation (4.33) becomes close to the original quantities $\boldsymbol{f}(t;\boldsymbol{x},\boldsymbol{z})$ (see Figure 5.7).

5.12 Discretization of PDE

In this section we will consider a one dimensional example ($d = 1$) where particles of the material will be organized in a certain way. This assumption is a restriction on the initial and boundary conditions of the original problem and is not implied by other factors.

Define $\mathcal{S} = [0, 1]$ and let $\Omega \subset \mathbb{R}$ be a bounded set. Suppose that $\chi : [0, T] \times \mathcal{S} \to \Omega$ is a smooth differentiable function, and for any $t \in [0, T]$ and $s \in \operatorname{int}(\mathcal{S})$ function χ satisfies

$$M\ddot{\chi}(t, s) = \frac{d}{ds}U'(\partial_s\chi(t, s)) \tag{5.40}$$

for some potential U.

Next, consider a system of N particles defined by

$$q_j(t) = \chi(t, s_j), \qquad s_j = \frac{j}{N} = j\varepsilon$$

where $q_j(t)$ is the position of i-th particle at the moment t ($j = 1 \dots N$) and $\varepsilon = N^{-1}$. Given the expression for the position of particles, we can find the representation of the velocities and accelerations:

$$v_j(t) = \dot{q}_j(t) = \dot{\chi}(t, s_j), \qquad a_i(t) = \ddot{q}_j(t) = \ddot{\chi}(t, s_j)$$

Next, observe that $\kappa_{i,i+1}$ has the form

$$\kappa_{j,j+1} = \frac{q_j(t) - q_{j+1}(t)}{\varepsilon} = \frac{\chi(t, s_j) - \chi(t, s_j + \varepsilon)}{\varepsilon} = -\partial_s\chi(t, s_j) + R_\kappa(t, s_j, \varepsilon)$$

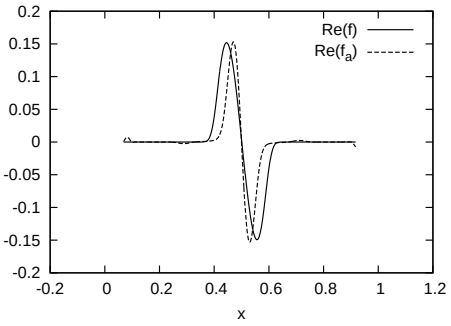

(a) Re $\boldsymbol{f}_\eta^\tau(t;\boldsymbol{x},\boldsymbol{z})$ and real of (4.33)

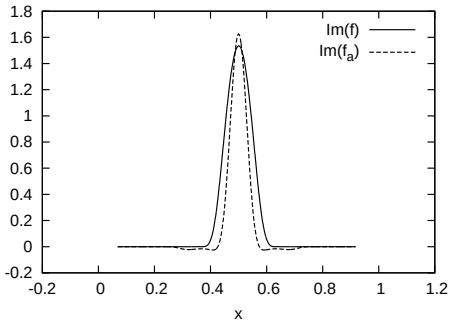

(b) Im $\boldsymbol{f}_\eta^\tau(t;\boldsymbol{x},\boldsymbol{z})$ and imag. of (4.33)

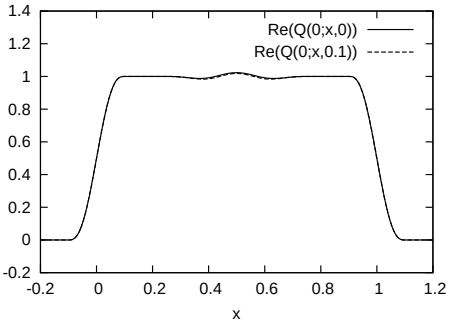

(c) Re$(Q_\eta^\tau(0;\boldsymbol{x},\boldsymbol{z}))$

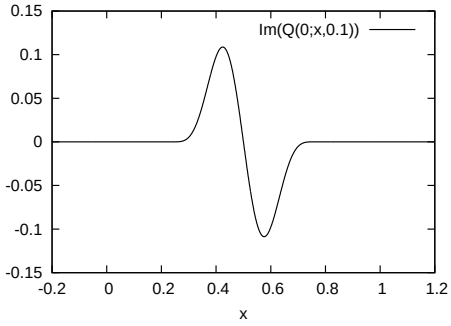

(d) Im$(Q_\eta^\tau(0;\boldsymbol{x},\boldsymbol{z}))$

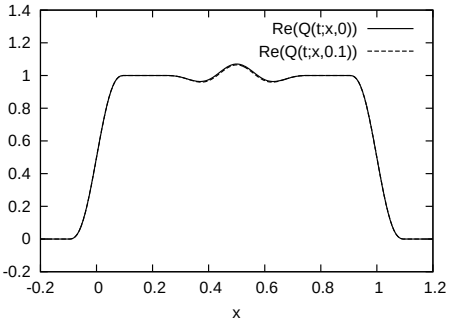

(e) Re$(Q_\eta^\tau(t^\star;\boldsymbol{x},\boldsymbol{z}))$

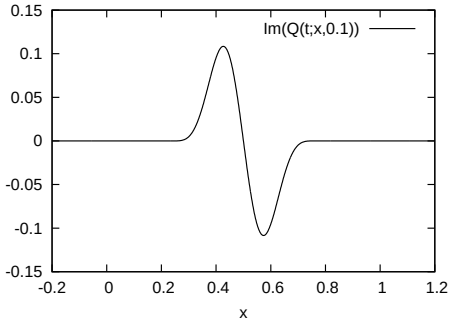

(f) Im$(Q_\eta^\tau(t^\star;\boldsymbol{x},\boldsymbol{z}))$

Figure 5.7: Results of numerical simulations

where $R_\kappa(t, s_j, \varepsilon)$ is

$$R_\kappa(t, s_j, \varepsilon) = -\frac{1}{2}\partial_s^2\chi(t, \sigma_i)\varepsilon, \qquad \sigma_i \in [s_j, s_{j+1}]$$

and, hence, $R_\kappa(t, s_j, \epsilon) \to 0$ as $N \to \infty$, since $\partial_s^2\chi(t, \sigma_i)$ is bounded. Continuity of U' implies

$$\lim_{N\to\infty} U'(\kappa_{j,j+1}) = U'(\lim_{N\to\infty} \kappa_{j,j+1}) = U'(-\partial_s\chi(t, s_j))$$

and, therefore, the force between two particles approaches $U'(-\partial_s\chi(t, s_j))$. Next, assume that $\operatorname{supp} U \subset (-r, r)$, and for all j and t we have

$$\frac{r}{2} < \partial_s\chi(t, s_j) < r,$$

then every particle will interact only with its direct neighbors. Indeed,

$$\begin{aligned}\kappa_{j,j+2} &= \frac{q_j(t) - q_{j+2}(t)}{\varepsilon} = \frac{q_j(t) - q_{j+1}(t)}{\varepsilon} + \frac{q_{j+1}(t) - q_{j+2}(t)}{\varepsilon} \\ &= -\partial_s\chi(t, s_j) - \partial_s\chi(t, s_i + \epsilon) + R_\kappa(t, s_j, \epsilon) + R_\kappa(t, s_{j+1}, \epsilon)\end{aligned}$$

and by continuity of $\partial_s\chi(t, s)$ we have

$$\lim_{N\to\infty} \partial_s\chi(t, s_j + \epsilon) = \partial_s\chi(t, s_j).$$

Therefore,

$$\lim_{N\to\infty} \kappa_{j,j+2} = -2\partial_s\chi(t, s_j) < -r$$

and for sufficiently large values of N we have $U'(\kappa_{j,j+2}) = 0$.

Consider the definition (3.22) of quantity $Q_\eta(t; \boldsymbol{x}, \boldsymbol{z})$ applied to this system

$$Q_\eta(t; \boldsymbol{x}, \boldsymbol{z}) = \frac{M}{N}\sum_{j=1}^{N} e^{i\dot\chi(t,s_j)\cdot\boldsymbol{z}}\psi_\eta(\boldsymbol{x} - \chi(t, s_j)) \tag{5.41}$$

and the definition (3.24) of $\boldsymbol{f}_\eta(t; \boldsymbol{x}, \boldsymbol{z})$:

$$\boldsymbol{f}_\eta(t; \boldsymbol{x}, \boldsymbol{z}) = \frac{M}{N}\sum_{j=1}^{N} \ddot\chi(t, s_j)e^{i\dot\chi(t,s_j)\cdot\boldsymbol{z}}\psi_\eta(\boldsymbol{x} - \chi(t, s_j)) \tag{5.42}$$

Observe that (5.41) and (5.42) are Riemann sums, so that as N approaches infinity we have

$$\lim_{N\to\infty} Q_\eta(t;\boldsymbol{x},\boldsymbol{z}) = M\int_{\mathcal{S}} e^{i\dot\chi(t,s)\cdot\boldsymbol{z}}\psi_\eta(\boldsymbol{x}-\chi(t,s))ds \tag{5.43}$$

$$\lim_{N\to\infty} \boldsymbol{f}_\eta(t;\boldsymbol{x},\boldsymbol{z}) = M\int_{\mathcal{S}} \ddot\chi(t,s)e^{i\dot\chi(t,s)\cdot\boldsymbol{z}}\psi_\eta(\boldsymbol{x}-\chi(t,s))ds \tag{5.44}$$

Let us change the variable of integration in (5.43) and (5.44). Define $u=\chi(t,s)$. Then

$$s=\chi^{-1}(t,u), \qquad ds=\partial_{\boldsymbol{x}}\chi^{-1}(t,u)du$$

and

$$\lim_{N\to\infty} Q_\eta(t;\boldsymbol{x},\boldsymbol{z}) = M\int_{\mathcal{S}} e^{i\dot\chi(t,\chi^{-1}(t,u))\cdot\boldsymbol{z}}\psi_\eta(\boldsymbol{x}-u)\partial_{\boldsymbol{x}}\chi^{-1}(t,u)du \tag{5.45}$$

$$\lim_{N\to\infty} \boldsymbol{f}_\eta(t;\boldsymbol{x},\boldsymbol{z}) = M\int_{\mathcal{S}} \ddot\chi(t,s)e^{i\dot\chi(t,\chi^{-1}(t,u))\cdot\boldsymbol{z}}\psi_\eta(\boldsymbol{x}-u)\partial_{\boldsymbol{x}}\chi^{-1}(t,u)du \tag{5.46}$$

Next, consider the limit of (5.45) and (5.46) as $\eta\to 0$. As $\eta\to 0$, the integrals in (5.45) and (5.46) become mollification. Therefore,

$$Q(t;\boldsymbol{x},\boldsymbol{z}) = \lim_{\eta\to 0}\lim_{N\to\infty} Q_\eta(t;\boldsymbol{x},\boldsymbol{z}) = Me^{i\dot\chi(t,\chi^{-1}(t,x))\cdot z}\partial_x\chi^{-1}(t,x), \tag{5.47}$$

$$\boldsymbol{f}(t;\boldsymbol{x},\boldsymbol{z}) = \lim_{\eta\to 0}\lim_{N\to\infty} \boldsymbol{f}_\eta(t;\boldsymbol{x},\boldsymbol{z}) = M\ddot\chi(t,\chi^{-1}(t,x))e^{i\dot\chi(t,\chi^{-1}(t,x))\cdot z}\partial_x\chi^{-1}(t,x) \tag{5.48}$$

Simplify the right hand side of (5.40)

$$\frac{d}{ds}U'(\partial_s\chi(t,s)) = U''(\partial_s\chi(t,s))\partial_s^2\chi(t,s)$$

Using (5.40) and the equality above rewrite (5.48) in the form

$$\boldsymbol{f}(t;\boldsymbol{x},\boldsymbol{z}) = U''(\partial_s\chi(t,\chi^{-1}(t,x)))\partial_s^2\chi(t,\chi^{-1}(t,x))e^{i\dot\chi(t,\chi^{-1}(t,x))\cdot z}\partial_x\chi^{-1}(t,x) \tag{5.49}$$

Observe that

$$\partial_s\chi(t,\chi^{-1}(t,\boldsymbol{x})) = \frac{1}{\partial_{\boldsymbol{x}}\chi^{-1}(t,\boldsymbol{x})}$$

and

$$Q(t;\boldsymbol{x},0) = M\partial_{\boldsymbol{x}}\chi^{-1}(t,\boldsymbol{x})$$

Further, we have

$$\begin{aligned}\partial_{\boldsymbol{x}}Q(t;\boldsymbol{x},0) &= -\frac{1}{(\partial_s\chi(t,\chi^{-1}(t,\boldsymbol{x}))^2}\partial_s^2\chi(t,\chi^{-1}(t,\boldsymbol{x}))\partial_{\boldsymbol{x}}\chi^{-1}(t,\boldsymbol{x}) \\ &= -Q(\boldsymbol{x},0)^3\partial_s^2\chi(t,\chi^{-1}(t,\boldsymbol{x}))\end{aligned}$$

Thus, (5.49) can be rewritten as

$$\boldsymbol{f}(t;\boldsymbol{x},\boldsymbol{z}) = -Q(t;\boldsymbol{x},\boldsymbol{z})U''(MQ(t;\boldsymbol{x},0)^{-1})\frac{\partial_{\boldsymbol{x}}Q(t;\boldsymbol{x},0)}{Q(t;\boldsymbol{x},0)^3}$$

or

$$\boldsymbol{f}(t;\boldsymbol{x},\boldsymbol{z}) = \frac{Q(t;\boldsymbol{x},\boldsymbol{z})}{\rho(t;\boldsymbol{x})}\frac{d}{d\boldsymbol{x}}\left\{U'\left(\frac{M}{\rho(t;\boldsymbol{x})}\right)\right\} \tag{5.50}$$

Formula (5.50) provides a closure which becomes asymptotically exact as $N \to \infty$.

Theorem 3. *Closure (4.33) is exactly (5.50) in the context of the current section with the constants* $\alpha_1 = \alpha_2 = 1$ *and* $\beta_1 = \beta_2 = M$.

Proof. First, observe that in the context of this section

$$Q(t;\boldsymbol{x},\boldsymbol{z}) = \rho(t;\boldsymbol{x})e^{iz\frac{\boldsymbol{p}(t;\boldsymbol{x})}{\rho(t;\boldsymbol{x})}}$$

and, therefore,

$$\frac{Q(t;\boldsymbol{x},\boldsymbol{z})}{\rho(t;\boldsymbol{x})} = e^{iz\frac{\boldsymbol{p}(t;\boldsymbol{x})}{\rho(t;\boldsymbol{x})}}$$

Differentiating both sides of the equality, we find

$$\frac{d}{d\boldsymbol{x}}\left\{\frac{Q(t;\boldsymbol{x},\boldsymbol{z})}{\rho(t;\boldsymbol{x})}\right\} = e^{iz\frac{\boldsymbol{p}(t;\boldsymbol{x})}{\rho(t;\boldsymbol{x})}}iz\frac{d}{d\boldsymbol{x}}\left\{\frac{\boldsymbol{p}(t;\boldsymbol{x})}{\rho(t;\boldsymbol{x})}\right\} = iz\frac{Q(t;\boldsymbol{x},\boldsymbol{z})}{\rho(t;\boldsymbol{x})}\frac{d}{d\boldsymbol{x}}\left\{\frac{\boldsymbol{p}(t;\boldsymbol{x})}{\rho(t;\boldsymbol{x})}\right\} \tag{5.51}$$

Finally, simplifying (4.33) using (5.51) we complete the proof. □

CHAPTER SIX

BI-STABLE MATERIALS

6.13 Introduction

This chapter presents an example of a particle system that can be studied with the method proposed in the thesis. This example is a simple discrete model of phase transition. We study deformation of two-dimensional *bistable lattices* (BL), periodic triangular networks of bistable elastic rods. A similar network with linearly elastic rods has been used by Cauchy, who formally averaged this assembly and obtained the first equations of continuum elasticity [12]. We consider a similar assembly, assuming that the rods are bistable. The bistability models a phase transition: It is assumed that each rod has two equilibrium lengths l and $l(1+s)$, respectively. Here, s can vary between $\frac{1}{2}$ and 2, so that the triangle inequality holds and a triangle of transformed rods still remains a triangle. This bistable lattice model is a simple finite dimensional model for phase transitions in solids. It allows for detailed description of inhomogeneous deformations and does not involve any tacit assumptions of the continuum theory. Here, the lattice is considered as a primary object and not as a discretization of a continuum. Although it does not have all the features of continuum, it captures most of them.

The considered lattices also model special protective structures. The wire meshes with bistable *waiting links* are used for protective structures because they have larger impact resistivity than a similar standard lattice, see [5, 21]. To achieve bimodality, one uses the links made of two different rods with welded ends (one rode is slightly longer than the other and, hence, slightly curved). First, the shorter (basic) rod resists the elongation alone, then a damage or fracture develops in it and its resistivity decreases, then the second (waiting) rod straightens, starts to resist and the total resistivity increases again. The resulting force versus elongation curve is non-monotone: First it increases, then decreases, and then increases again. The corresponding energy is bimodal. The bimodal link structures can sustain a large impact because a significant portion of its energy is spent to break the basic links. The lattice recovers the resistivity at a different equilibrium states due to bimodality. The chapters [8, 7] demonstrate the superior resistivity of the regular triangular

lattice. In order to rupture it, one must break the basic rods in a large portion of structure spending much more energy than it is needed to break a similar conventional lattice. The bistable structures delocalize the damage: the partially broken links are spread over a large area.

One dimensional chains of bistable rods are well investigated [1, 2, 19, 20, 24, 25]. Some results on the two-dimensional bistable lattices can be found in [17, 18] (explicit construction of certain special solutions, discrete Green functions), and [6, 7] (direct numerical simulations of time-dependent impact fracture problems). Other related problems are treated in the book [22] that also contains additional references.

The partially bistable damaged lattice is composed of short and long links. Its deformation is inhomogeneous, and it does not satisfy the Cauchy-Born rule, see [9]. However, we assume that the structure regains periodicity and starts to follow Cauchy-Born rule at a much larger scale. The continuum limit corresponds to the infinite period. Two scales are introduced: The scale of a single rod and of the period. The external load is still assumed to be homogeneous in the scale of period. Implicitly, an even larger scale is assumed to account for inhomogeneity of the load and boundary conditions.

Section 6.14 contains formulation of the problem and derivation of the compatibility conditions. We consider compatibility of the "long" and "short" rods in a lattice. The transition of links to a new state generally leads to an elastic deformation of all rods. For example, one transformed (elongated) rod does not fit into a triangular lattice of nontransformed (short) links without distorting the lattice and increasing the energy of the assembly. The partially damaged lattice possesses many equilibria. Some of equilibria (called here *still states*) correspond to nonstressed state of the whole lattice and zero energy. Notice that the resistivity of the structure in a damaged still state is equal to the resistivity of the undamaged structure, but the energy of an impact is absorbed during the transition to that state. In Section 6.16 we introduce still states. We show that there exists a class of still structures that densely cover the neutral region, and describe the corresponding set of eigenvalues. In Section 6.17, we formulate the linearized problem, assuming that the two equilibrium lengths are close to each other. A formula for average strain is obtained in Section 6.18, it expresses strain in terms of rod elongations. In Section 6.20, we show that the compatibility conditions are necessary and sufficient for existence of a lattice deformation realizing a given set of rod elongations. In Section 6.21, we prove a characterization theorem for the neutral region $\mathcal{D}$.

This is done by constructing a certain family of still states called *stripes*. The eigenstrains of the stripes fill $\mathcal{D}$ densely, in the sense that every strain within this set can be approximated by an average strain of some stripe, with an error of order $N^{-1/2}$ where N is the number of nodes.

6.14 The problem

6.14.1 Energy of one bistable rod

Consider a bistable elastic rod with the energy $W_r(x)$ that possesses two equal minima $W_r(l) = W_r((1+s)l) = 0$. Let us also assume that $W_r(x)$ is convex outside of the interval $[l,\ l(1+s)]$, and its second derivative is positive in a proximity of each minima $x = l$ and $x = l(1+s)$. For definiteness, we may assume that the dependence of $W_r(x)$ on the length $x > 0$ is piece-wise quadratic (W_r^q) or polynomial (W_r^p)

$$W_r^q(x) = \min\left\{\frac{1}{2}(x-l)^2, \frac{1}{2}C(x-l(1+s))^2\right\}, \tag{6.52}$$

$$W_r^p(x) = (x-l)^2(x-l(1+s))^2, \tag{6.53}$$

where l is the length of the rod in the reference configuration, $l+s$ is the length in the elongated mode, and $\frac{1}{2} < 1+s < 2$.

The rods are elastic and locally stable in a proximity of the equilibria. The elastic force f_r in the rod is

$$f_r(x) = \frac{dW_r}{dx}.$$

The rod has two equilibrium states $x = l$ and $x = l(1+s)$ of equal energy

$$f_r(x) = 0, \quad W_r(x) = 0 \quad \text{if } x = l,\ l(1+s).$$

The magnitude of the force monotonically increases with the elongation l in the proximity of equilibria.

There are several equilibrium lengths x_α and x_β for every f_r in a proximity of zero. They are solutions of the equation

$$\frac{dW_r}{dx} = 0$$

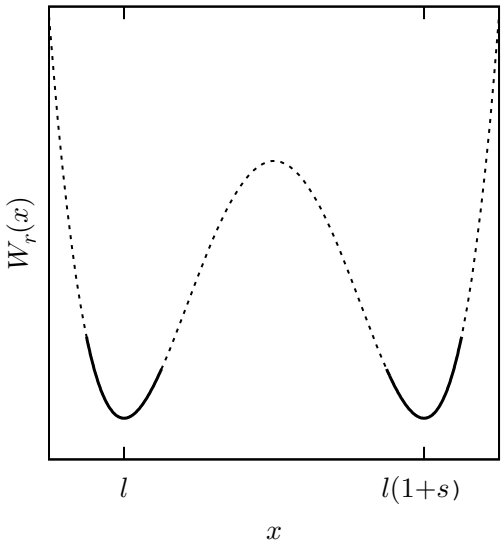

Figure 6.8: Energy of a bistable rod

6.14.2 Triangular network

Consider a triangular periodic network made of the links defined above. For each node, there are six rods joining it with six neighbors. When the rods are of equal lengths, the network is elastically isotropic. The number of nodes in the period is three times less than the number of rods between them. There are three families of the parallel rods in the network

When the rods transit to a different state, the network becomes inhomogeneous (each rod can have a different length). We assume that the transition is periodic. Each period consists of N nodes where N can be arbitrary large. The network's energy is the sum of energies stored in all $3N$ links. The length of a link can be expressed through the position of its ends, that is the nodes. The nodes are determined by N pairs of coordinates in a plane, or by $2N$ parameters. Hence, the links' lengths can not be arbitrary (for example, see Figure 6.9(a)). We conclude that they are subject to N *compatibility conditions* that we derive now.

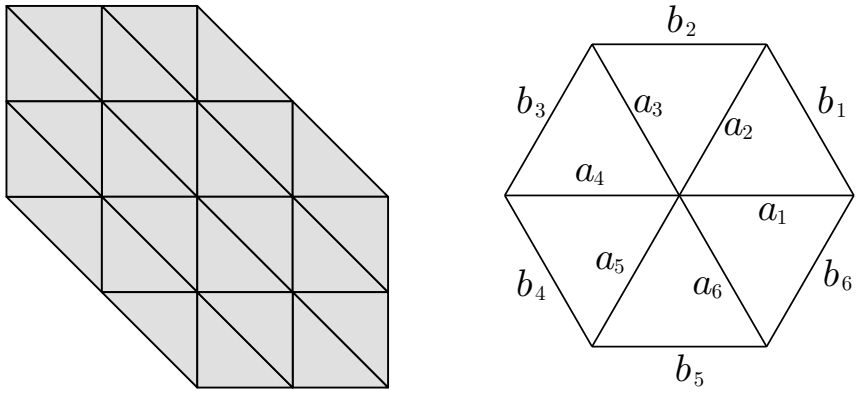

(a) Compatible structure (b) Hexagonal block

Figure 6.9: Compatibility of link lengths

6.15 Compatibility conditions

6.15.1 Necessary condition

There are conditions that constrain the lengths of the rods that can be joined in a hexagonal lattice. Consider an inner node in the lattice. There are six rods that link the node with its neighbors; let us denote the lengths of them as $a_1, \dots a_6$ (see figure 6.9(b)). Consider also six rods that surround the node forming a hexagon around it; let us denote the lengths of them as $b_1, \dots b_6$. These rods form six triangles joined at the node. The angles at the node will be denoted by $\phi_1, \dots, \phi_6$.

The lengths of the listed twelve rods cannot be arbitrary. The sum of angles of the six triangles should be equal to 2π,

$$\sum_{i=1}^{6} \phi_i = 2\pi. \tag{6.54}$$

To express this condition in terms of the lengths, we use trigonometry. Cosine of each angle ϕ_i is expressed through the lengths of the links as

$$\cos(\phi_i) = \frac{a_i^2 + a_{i+1}^2 - b_i^2}{2a_i a_{i+1}}, \quad i = 1, \dots, 6. \tag{6.55}$$

Here, $a_7 = a_1$. Therefore, the lengths of rods are constrained as follows

$$\sum_{i=1}^{6} \arccos\left(\frac{a_i^2 + a_{i+1}^2 - b_i^2}{2a_i a_{i+1}}\right) = 2\pi. \tag{6.56}$$

The number of these constraints is equal to the number of inner nodes in the structure.

6.15.2 Linearized compatibility conditions

In a linearized case when the lengths of the rods are close to l, constraints (6.56) are simplified. Assuming that

$$a_i = l(1+\kappa_{a_i}), \quad b_i = l(1+\kappa_{b_i}), \quad i = 1,\dots,6 \tag{6.57}$$

we write ϕ_i as the function of κ_{a_i}, $\kappa_{a_{i+1}}$, κ_{b_i}:

$$\phi_i = \arccos \frac{(1+\kappa_{a_i})^2 + (1+\kappa_{a_{i+1}})^2 - (1+\kappa_{b_i})^2}{2(1+\kappa_{a_i})(1+\kappa_{a_{i+1}})}.$$

Linearizing near

$$\begin{pmatrix} \kappa_{a_i} \\ \kappa_{a_{i+1}} \\ \kappa_{b_i} \end{pmatrix} = \begin{pmatrix} 0 \\ 0 \\ 0 \end{pmatrix}$$

we find

$$\sum_{i=1}^{6} \phi_i = 2\pi + \frac{\sqrt{3}}{3}\left(\sum_{i=1}^{6} \kappa_{a_i} + \sum_{i=1}^{6} \kappa_{a_{i+1}} - 2\sum_{i=1}^{6} \kappa_{b_i}\right)$$

Substituting this expression into (6.54), we obtain an elegant *linearized compatibility condition for lattices*

$$\sum_{i=1}^{6} \kappa_{a_i} = \sum_{i=1}^{6} \kappa_{b_i} \tag{6.58}$$

It states that the sum of the elongations of the spokes that come out of a node is equal to the elongation of the hexagonal rim around this node.

6.16 Definitions

In this section we consider *still configurations*. These are deformed states with zero force in each rod. Because of the force-elongation dependence, this requires the length of each rod to be either l or $l(1+s)$. To simplify presentation, in this section we scale $l = 1$ and denote $l(1+s) = a$. Given a collection of such rod lengths, we call a configuration *still* if it is geometrically compatible, that is the ends of the link of the length one and a can meet in the nodes. The examples of still

configurations are given below in Figure 6.10. We recall that eigenstrain is a generic name given to various non-elastic strains, such as strains due to thermal expansion, phase transformation, initial strains and so on.

Notice that the problem is reduced to a geometric problem of *tiling* of the plane with triangles of four types with the lengths of the sides being equal to $\{1,1,1\}$, $\{1,1,a\}$, $\{1,a,a\}$. and $\{a,a,a\}$, respectively.

We work with small elongations ($a \approx 1$), so it makes sense to linearize rod elongations near the reference configuration. Linear description allows us to use all tools of linear algebra, so all proofs become easier and more elegant.

6.17 Linearized elongations

The linearized relative elongation κ_{ij} of the rod (i,j) can be written as

$$\kappa_{ij} = \boldsymbol{q}_{ij} \cdot \frac{\boldsymbol{u}_j - \boldsymbol{u}_i}{l}, \tag{6.59}$$

where $\boldsymbol{q}_{ij}$ is the unit direction from node i to node j in the reference configuration, $\boldsymbol{u}_i$ and $\boldsymbol{u}_j$ are the displacements of nodes i and j, respectively.

Consider a triangular periodic network of N nodes, where N is finite, even though it can be arbitrary large. We also suppose that the nodes are arranged into a hexagonal shape containing n nodes along a side (see Figure 5.1 for an example).

Factoring out l^2 in (6.52) and using nodal displacements instead of the rod length, we write the energy of a rod (i,j) as

$$w(\kappa_{ij}) = \frac{Cl^2}{2} \min\{\kappa_{ij}^2, (\kappa_{ij} - s)^2\}, \tag{6.60}$$

where, $s > 0$ is a dimensionless parameter characterizing the critical relative elongation. The graph of the dependence $w(\kappa_{ij})$ is shown on figure 6.11 (Compare with (6.52), where x denotes the actual rod length).

The displacements u_k in the equilibrium state are found by minimizing the total energy of the

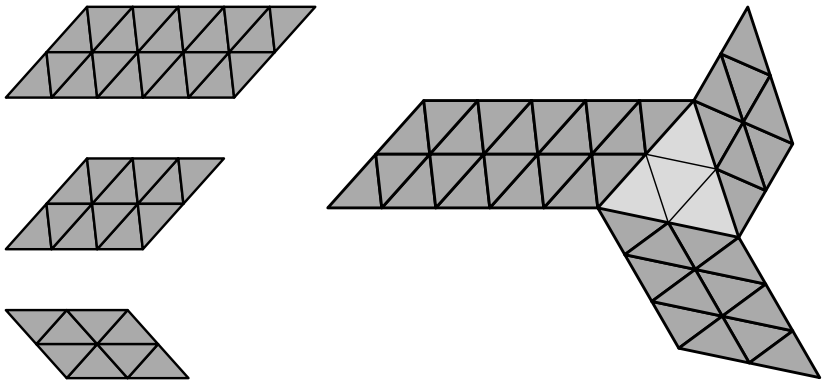

(a) Step 1

(b) Step 2

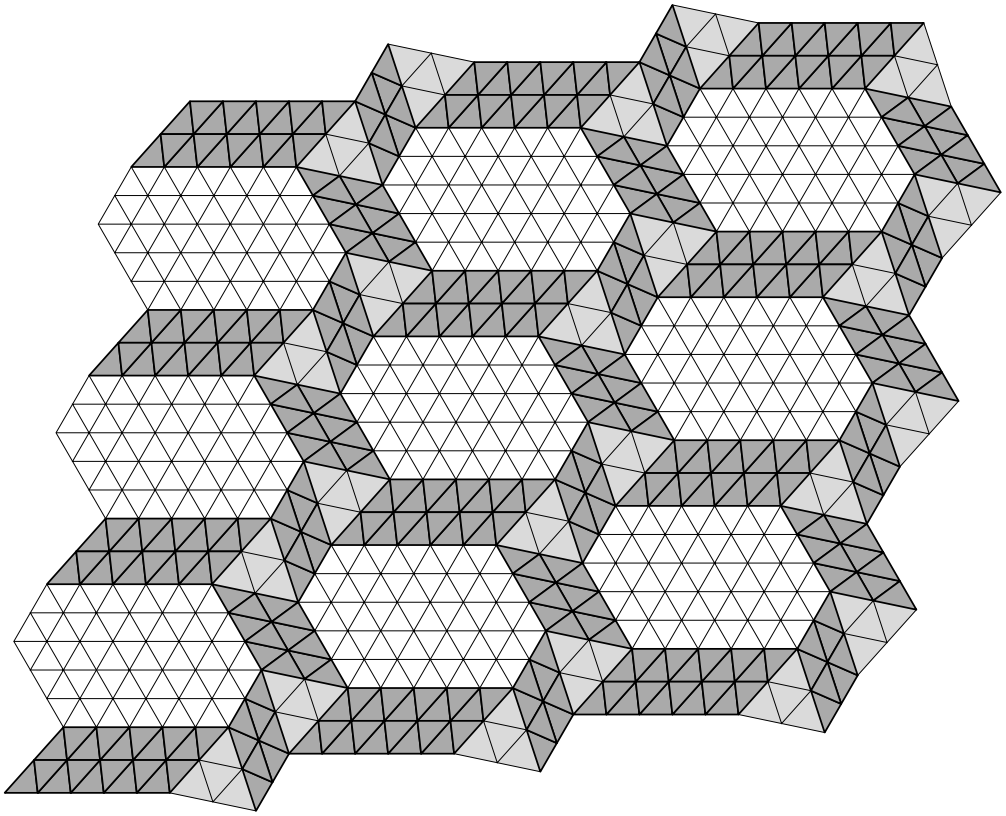

(c) Step 3, the structure

Figure 6.10: Hexagon-triangle strips and the assembly

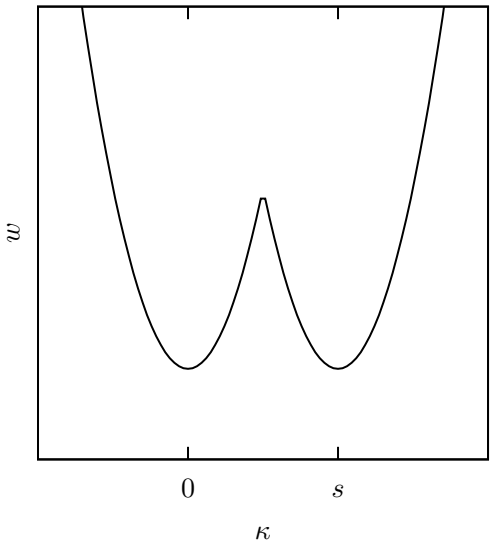

Figure 6.11: Energy of a single rod

network:

$$W(\boldsymbol{u}_1, \dots \boldsymbol{u}_N) = \sum_{(i,j)} w(\kappa_{ij}) = \sum_{(i,j)} w\left(\boldsymbol{q}_{ij} \cdot \frac{\boldsymbol{u}_j - \boldsymbol{u}_i}{l}\right)$$

6.18 Average strain

An effective homogeneous deformation state of the network is characterized by an average (linearized) strain tensor $\boldsymbol{E}$. In this section we obtain a formula for the average strain in terms of elongations κ_{ij}.

Denote the number of nodes in the network by N. Given a set of displacements of nodes $\boldsymbol{u}_1, \dots \boldsymbol{u}_N$ we define a continuum deformation $\boldsymbol{u}(x)$ that coincides with $\boldsymbol{u}_i$ at each $\boldsymbol{x}_i$. This can be done by interpolating. In the present case, the lattice forms a triangulation of the physical domain Ω. Therefore it is easy to construct a piecewise linear interpolant, using finite elements. After this is done we obtain a continuous function $\boldsymbol{u}(\boldsymbol{x}), \boldsymbol{x} \in \Omega$ such that

- $\boldsymbol{u}(\boldsymbol{x}_i) = \boldsymbol{u}_i$ for $i = 1, \dots N$ and $\boldsymbol{x}_i$ being the position of node i;
- $\boldsymbol{u}(\boldsymbol{x})$ is linear on every elementary triangle of the lattice.

To $\boldsymbol{u}(\boldsymbol{x})$ we associate strain tensor $\boldsymbol{\varepsilon}$:

$$\boldsymbol{\varepsilon} = \frac{\nabla \boldsymbol{u} + (\nabla \boldsymbol{u})^T}{2}$$

Average strain $\boldsymbol{E}$ is defined by the formula

$$\boldsymbol{E} = \frac{1}{|\Omega|} \int_\Omega \boldsymbol{\varepsilon}(\boldsymbol{x}) d\boldsymbol{x}, \tag{6.61}$$

where Ω is the domain of $\boldsymbol{u}$ and $|\Omega|$ is

$$|\Omega| = \int_\Omega d\boldsymbol{x}$$

There exist formulas for $\boldsymbol{E}$ in terms of displacements $\boldsymbol{u}_i$ (see [4], [15]). However, for our purposes it is better to work with the relative elongations κ_{ij} because we would often prescribe elongations, rather than displacements. To use standard formulas one would have to solve the system (6.69) (see the next section) that relates elongations and displacements. We choose a more direct route that involves relating three average elongations along the lattice directions with the three independent components of the average strain.

Rewrite (6.61) as

$$\boldsymbol{E} = \frac{1}{|\Omega|} \int_\Omega \boldsymbol{\varepsilon}(\boldsymbol{x}) d\boldsymbol{x} = \frac{1}{|\mathcal{T}|} \sum_{\Delta \in \mathcal{T}} \boldsymbol{\varepsilon}_\Delta,$$

where $\mathcal{T}$ is the set of elementary triangles of the network, $|\mathcal{T}|$ is the number of elementary triangles in the network, and $\boldsymbol{\varepsilon}_\Delta$ is the strain tensor on elementary triangle Δ:

$$\boldsymbol{\varepsilon}_\Delta = \frac{\nabla \boldsymbol{u}_\Delta + (\nabla \boldsymbol{u}_\Delta)^T}{2} = \frac{1}{|\Omega_\Delta|} \int_{\Omega_\Delta} \boldsymbol{\varepsilon}(\boldsymbol{x}) d\boldsymbol{x}$$

Since the average strain tensor $\boldsymbol{E}$ is a 2×2 symmetric matrix, it has three independent components:

$$\boldsymbol{E} = \begin{bmatrix} a & b \\ b & c \end{bmatrix}$$

Consider three lattice direction vectors $\boldsymbol{q}_1$, $\boldsymbol{q}_2$, and $\boldsymbol{q}_3$ (see figure 6.12(a)):

$$\boldsymbol{q}_1 = \frac{1}{2}\begin{bmatrix} 2 \\ 0 \end{bmatrix}, \quad \boldsymbol{q}_2 = \frac{1}{2}\begin{bmatrix} 1 \\ \sqrt{3} \end{bmatrix}, \quad \boldsymbol{q}_3 = \frac{1}{2}\begin{bmatrix} -1 \\ \sqrt{3} \end{bmatrix},$$

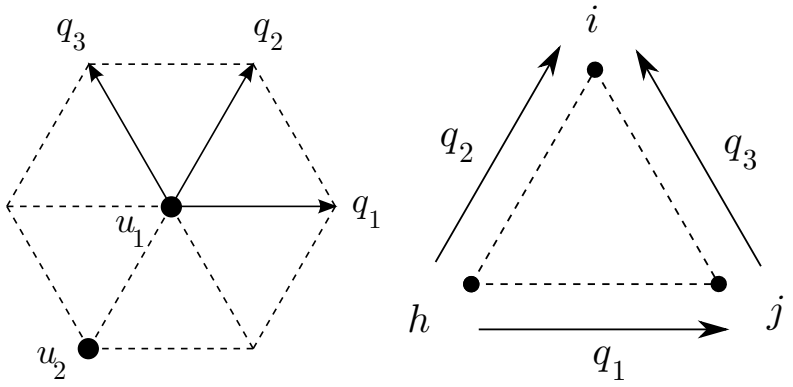

(a) Three lattice directions (b) Definition of vector $\boldsymbol{k}_\Delta$

Figure 6.12: Lattice directions

We can find the components of $\boldsymbol{E}$ using the values $\boldsymbol{q}_r \cdot (\boldsymbol{E}\boldsymbol{q}_r)$, $r = 1, 2, 3$. Observe that

$$\boldsymbol{q}_r \cdot (\boldsymbol{E}\boldsymbol{q}_r) = \frac{1}{|\mathcal{T}|}\sum_{\Delta\in\mathcal{T}} \boldsymbol{q}_r \cdot (\boldsymbol{\varepsilon}_\Delta \boldsymbol{q}_r) = \frac{1}{|\mathcal{T}|}\sum_{\Delta\in\mathcal{T}} \boldsymbol{q}_r \cdot (\nabla \boldsymbol{u}_\Delta \boldsymbol{q}_r). \tag{6.62}$$

Using linearity of $\boldsymbol{u}$ on triangle Δ for edge (i, j) of the triangle we find

$$\boldsymbol{q}_{ij} \cdot (\boldsymbol{\varepsilon}_\Delta \boldsymbol{q}_{ij}) = \boldsymbol{q}_{ij} \cdot (\nabla \boldsymbol{u}_\Delta \boldsymbol{q}_{ij}) = \boldsymbol{q}_{ij} \cdot \frac{\boldsymbol{u}_j - \boldsymbol{u}_i}{l} = \kappa_{ij}$$

Given a triangle Δ with vertices h, i, j (see figure 6.12(b)) define vector $\boldsymbol{k}_\Delta \in \mathbb{R}^3$ as:

$$\boldsymbol{k}_\Delta = \begin{bmatrix} \kappa_{hj} \\ \kappa_{hi} \\ \kappa_{ij} \end{bmatrix}$$

Using this notation we rewrite (6.62) as a linear system for finding the components a, b, c of $\boldsymbol{E}$

given elongations κ_{ij}:

$$Q \begin{bmatrix} a \\ b \\ c \end{bmatrix} = \frac{1}{|\mathcal{T}|} \sum_{\Delta \in \mathcal{T}} \boldsymbol{k}_\Delta, \tag{6.63}$$

where the matrix Q is given by

$$Q = \begin{bmatrix} q_{1,1}^2 & 2q_{1,1}q_{1,2} & q_{1,2}^2 \\ q_{2,1}^2 & 2q_{2,1}q_{2,2} & q_{2,2}^2 \\ q_{3,1}^2 & 2q_{3,1}q_{3,2} & q_{3,2}^2 \end{bmatrix} = \begin{bmatrix} 1 & 0 & 0 \\ \frac{1}{4} & \frac{\sqrt{3}}{2} & \frac{3}{4} \\ \frac{1}{4} & -\frac{\sqrt{3}}{2} & \frac{3}{4} \end{bmatrix} \tag{6.64}$$

Define function $\mathrm{m} : \mathbb{R}^3 \to \mathbb{R}^{2\times 2}$ by

$$\mathrm{m}(\boldsymbol{x}) = \boldsymbol{x}_1 \begin{bmatrix} 1 & 0 \\ 0 & 0 \end{bmatrix} + \boldsymbol{x}_2 \begin{bmatrix} 0 & 1 \\ 1 & 0 \end{bmatrix} + \boldsymbol{x}_3 \begin{bmatrix} 0 & 0 \\ 0 & 1 \end{bmatrix}$$

Function m is simply a linear 1-1 mapping from the space of three dimensional vectors to the space of 2×2 symmetric matrices.

Solving (6.63) we find average strain $\boldsymbol{E}$:

$$\boldsymbol{E} = \frac{1}{|\mathcal{T}|} \mathrm{m}\left(Q^{-1} \sum_{\Delta \in \mathcal{T}} \boldsymbol{k}_\Delta \right), \tag{6.65}$$

where

$$Q^{-1} = \begin{bmatrix} 1 & 0 & 0 \\ 0 & \frac{\sqrt{3}}{3} & -\frac{\sqrt{3}}{3} \\ -\frac{1}{3} & \frac{2}{3} & \frac{2}{3} \end{bmatrix}$$

Further, we will rewrite the sum over triangles in (6.65) as the sum over edges (this is just the change in indexing). Denote all edges of the array by $\mathcal{E}$, all boundary edges of the array by $\mathcal{E}_B$ and all non-boundary edges of the array by $\mathcal{E}_I$ ($\mathcal{E}_I = \mathcal{E} \backslash \mathcal{E}_B$). Then

$$\sum_{\Delta \in \mathcal{T}} \boldsymbol{k}_\Delta = 2 \sum_{e \in \mathcal{E}} \boldsymbol{k}_e - \sum_{e \in \mathcal{E}_B} \boldsymbol{k}_e,$$

where vector $\boldsymbol{k}_e \in \mathbb{R}^3$ has the components defined by

$$(\boldsymbol{k}_e)_r = \begin{cases} \kappa_e, & \text{if edge } e \text{ is parallel to } \boldsymbol{q}_r \\ 0, & \text{else} \end{cases}, \quad r = 1, 2, 3$$

Next, equation (6.65) can be rewritten as

$$\boldsymbol{E} = \frac{2}{|\mathcal{T}|} \mathrm{m} \left(Q^{-1} \sum_{e \in \mathcal{E}} \boldsymbol{k}_e \right) - \frac{1}{|\mathcal{T}|} \mathrm{m} \left(Q^{-1} \sum_{e \in \mathcal{E}_B} \boldsymbol{k}_e \right).$$

Denote the average elongation by $\bar{\boldsymbol{k}}$:

$$\bar{\boldsymbol{k}} = \frac{1}{|\mathcal{E}|} \sum_{e \in \mathcal{E}} \boldsymbol{k}_e. \tag{6.66}$$

Then we rewrite (6.65) and obtain the desired formula for the average strain in terms of average elongations:

$$\boldsymbol{E} = 2 \frac{|\mathcal{E}|}{|\mathcal{T}|} \mathrm{m}(Q^{-1} \bar{\boldsymbol{k}}) - \frac{1}{|\mathcal{T}|} \mathrm{m} \left(Q^{-1} \sum_{e \in \mathcal{E}_B} \boldsymbol{k}_e \right). \tag{6.67}$$

This formula is used extensively in the remainder of the chapter. The first term in the right hand side contains contributions from all interior edges of the lattice, while the second term contains the contributions from the boundary edges only. As the number of nodes increases, the second term becomes small comparing to the first. This becomes clear from the following estimate

$$\left\| m \left(\frac{1}{|\mathcal{T}|} Q^{-1} \sum_{e \in \mathcal{E}_B} \boldsymbol{k}_e \right) \right\|_F \leq \sqrt{2} \frac{|\mathcal{E}_B|}{|\mathcal{T}|} ||Q^{-1}||_2 \max_{e \in \mathcal{E}_B} ||\boldsymbol{k}_e||_2. \tag{6.68}$$

Here $\| \cdot \|_F$ denotes the Frobenius norm of a matrix, and $\| \cdot \|_2$ is the Euclidean norm. Note that the ratio

$$\frac{|\mathcal{E}_B|}{|\mathcal{T}|}$$

of the number of the boundary edges to the number of all elementary triangles goes to zero as the number of nodes approaches infinity.

6.19 Linearized compatibility conditions

In the next two sections, we study the linearized version of the problem of finding still states. The linearized formulation is as follows. Equations (6.59) relating node displacements with link elongations can be concisely written as

$$R\boldsymbol{U} = \boldsymbol{\kappa}, \tag{6.69}$$

where $\boldsymbol{U}$ is a tuple of displacements $\boldsymbol{u}_i$, say $(\boldsymbol{u}_1, \dots \boldsymbol{u}_N)$, and $\boldsymbol{\kappa}$ is a tuple of κ_{ij}. The number of unknowns in (6.69) is $2N$ (since each $\boldsymbol{u}_i$ has two independent components). The number of equations is larger, approximately $3N$ (see Lemma 5.1 below for the exact count). Therefore, we have an overdetermined system (the number of unknowns is less than the number of equations). As a consequence, (6.69) may be unsolvable for some $\boldsymbol{\kappa}$. The values of $\boldsymbol{\kappa}$ for which (6.69) is solvable are called *admissible*.

6.20 Compatibility conditions characterize range of R

In this section we show that compatibility conditions (6.58) are necessary and sufficient for solvability of (6.69). Necessity is clear from the derivation of (6.58), so we focus on sufficiency.

Suppose that we have the hexagonal array with a side of n points (see figure 6.13).

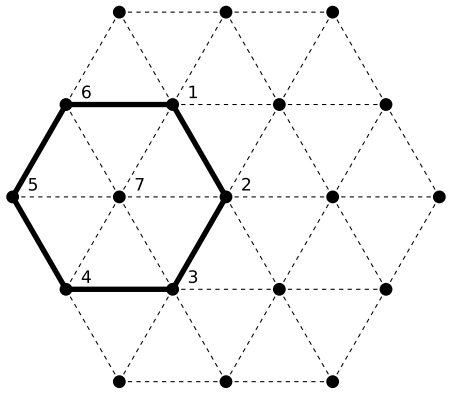

Figure 6.13: Example of the network with $N = 19$, $n = 3$. A hexagon that forms a hexagonal equations shown in bold

For every hexagon consisting of 6 vertices we formulate the condition (6.58): the sum of elongations of the outer edges equals to the sum of elongations of the inner edges. For example, for

figure 6.13 the equation will be

$$\kappa_{12} + \kappa_{23} + ... + \kappa_{56} + \kappa_{61} = \kappa_{71} + \kappa_{72} + ... + \kappa_{75} + \kappa_{76}$$

The collection of all such equations will be called *hexagonal equations*.

Next, we need a preliminary result giving the exact count of the number of nodes, edges and hexagonal equations. The following lemma is used later to carry out proofs by induction.

Lemma 3. *The total number of nodes N, the number of edges E, and the number of hexagonal equations M depend on n as follows.*

$$N(n) = 3n^2 - 3n + 1, \qquad E(n) = 9n^2 - 15n + 6, \qquad M(n) = 3n^2 - 9n + 7.$$

Proof. We will prove the lemma using mathematical induction.

For $n = 2$ we have a hexagon that has 7 vertices, 12 edges, and 1 hexagonal equation. Indeed,

$$N(2) = 3 \cdot 2^2 - 3 \cdot 2 + 1 = 7, \quad E(2) = 9 \cdot 2^2 - 15 \cdot 2 + 6 = 12, \quad M(2) = 3 \cdot 2^2 - 9 \cdot 2 + 7 = 1$$

Thus, the formulas are true for $n = 2$.

Suppose that given formulas are true for $n = k$. Let's prove that they are true for $n = k + 1$.

When we increase $n = k$ by 1 we "wrap" the array by a layer of points. Therefore, we add $6k$ vertices, we allow $6(k - 1)$ new hexagonal equations, and add $6(3k - 1)$ edges. Thus, the number of vertices N^* for the size $n = k + 1$ is:

$$\begin{aligned} N^* &= N(k) + 6k = 3k^2 - 3k + 1 + 6k = 3(k + 1 - 1)^2 + 3k + 1 \\ &= 3(k + 1)^2 - 6(k + 1) + 3 + 3k + 1 = 3(k + 1)^2 - 3(k + 1) + 1, \end{aligned}$$

the number of equations M^* is

$$\begin{aligned} M^* &= M(k) + 6(k - 1) = 3k^2 - 9k + 7 + 6(k - 1) = 3(k + 1 - 1)^2 - 3k + 1 \\ &= 3(k + 1)^2 - 6(k + 1) + 3 - 3k + 1 = 3(k + 1)^2 - 9(k + 1) + 7, \end{aligned}$$

and the number of edges E^* is

$$\begin{aligned} E^* &= E(k) + 6(3k-1) = 9k^2 - 15k + 6 + 18k - 6 = 9(k+1-1)^2 + 3k \\ &= 9(k+1)^2 - 18(k+1) + 9 + 3k = 9(k+1)^2 - 15(k+1) + 6, \end{aligned}$$

Since $N^* = N(k+1)$, $M^* = M(k+1)$, and $E^* = E(k+1)$, the formulas are true. □

Observe that

$$2N - 3 = E - M.$$

We know that for the mapping $R : \mathbb{R}^{2N} \to \mathbb{R}^E$ we have $\dim(\ker R) = 3$. This follows from the well known results on graph rigidity, in particular theorems on the first-order rigidity of triangulations (see e.g. [3] and references therein). Thus,

$$\dim(\text{im } R) = 2N - 3$$

The hexagonal equations can be concisely written in the form

$$Z\boldsymbol{\kappa} = 0, \tag{6.70}$$

where Z is a matrix, $Z : \mathbb{R}^E \to \mathbb{R}^M$; i-th row of this matrix corresponds to i-th equation.

Lemma 4. *Matrix Z has full rank M.*

Proof. We will restate the lemma in the form: all hexagonal equations are linearly independent.

We will prove the lemma in its new form using mathematical induction on n. For $n = 2$ we have $M = 1$. One equation is linearly independent.

Suppose, the lemma is true for $n = k$. Let's prove it for $n = k + 1$.

Increasing $n = k$ by 1 we wrap a hexagon of side size k with a layer of points. Doing so we add some number of hexagonal equations to those that we had in the original hexagon. The hexagonal equations of the original hexagon are linearly independent. Each new hexagonal equation contains an edge that is present in no other equation. Thus, all equations are linearly independent. □

Since matrix Z has rank M, we find $\dim(\ker Z) = E - M$. Thus,

$$\dim(\operatorname{Im} R) = \dim(\ker Z) \tag{6.71}$$

Necessity of hexagonal equations implies that each admissible $\boldsymbol{\kappa}$ satisfies them. This fact can be stated as follows: for any $\boldsymbol{\kappa} \in \operatorname{Im} R$ we have $Z\boldsymbol{\kappa} = 0$. This in turn implies

$$\text{im } R \subset \ker Z. \tag{6.72}$$

Theorem 4. *For any vector $\boldsymbol{\kappa} \in \mathbb{R}^E$ satisfying $Z\boldsymbol{\kappa} = 0$ there is a unique (up to translation and rotation) vector $\boldsymbol{u} \in \mathbb{R}^{2N}$ satisfying $R\boldsymbol{u} = \boldsymbol{\kappa}$.*

Proof. The conditions (6.71) and (6.72) imply

$$\operatorname{Im} R = \ker Z.$$

Thus, for any $\boldsymbol{\kappa} \in \mathbb{R}^E$ we can find a vector $\boldsymbol{u} \in \mathbb{R}^{2N}$. If we neglect rigid rotations and translations of the whole lattice (they form the null space of R by the well known results on rigidity of triangulations, ([3] and references therein), then this vector is unique. □

6.21 Still states and small deformation eigenstrains

In the small deformation case a still state is a collection of nodal displacements $\boldsymbol{u}_i$ satisfying equations (6.69) with the right hand side $\boldsymbol{\kappa}$ of special form. The components κ_{ij} can take only two values: 0 and s, where s is the critical elongation from (6.60). If $\kappa_{ij} = 0$ we call the corresponding edge (i, j) *short*, otherwise the edge is called *long*. To construct a still state, one could choose a length for each edge (long or short). The resulting configuration is accepted if the resulting triangles form a tessellation. Otherwise the configuration is rejected. In the case of small deformations, an admissible elongation vector $\boldsymbol{\kappa}$ should lie in the range of the matrix R from (6.69). Equivalently, such $\boldsymbol{\kappa}$ must be a solution of the hexagonal equations (6.70).

Denote the set of all still states by $\mathcal{U}$. To characterize $\mathcal{U}$, one needs to solve the following problem.

Given $\boldsymbol{\kappa}$ with $\boldsymbol{\kappa}_{ij} \in \{0, s\}$, find $\boldsymbol{U}$ realizing that $\boldsymbol{\kappa}$, that is, find $\boldsymbol{U}$such that $R\boldsymbol{U} = \boldsymbol{\kappa}$.

This is possible only if $\boldsymbol{\kappa}$ satisfies hexagonal equations from Section 6.19. Complete characterization of $\mathcal{U}$ seems very difficult, and is not addressed in this chapter. The reason for the difficulty is the lack of a convenient structure. It is easily checked that $\mathcal{U}$ is not a linear space, or even a convex set. Therefore, a description of this set cannot be obtained by linear algebra methods.

6.22 An algorithm of adding still states

In this section we characterize the set of strains that can be well approximated by the average strains of still states. An average strain of a still state can be conveniently described by a triple of concentrations of long edges parallel to the lattice directions. In this section we propose an explicit construction that furnishes a large number of still states. Concentrations of these states densely fill a certain unit cube in the concentration space. Our construction is based on two observations. First, one needs a binary operation that produces new still states by combining two already known still states. Second, one needs a simple "building block", that is, a still state that could be easily combined with its slightly modified (e.g. translated and rotated) replicas. In view of the linear structure of $\operatorname{im} R$, the convenient operation is summation. However, summation of two still states does not always produce a still state. An additional condition that ensures that the sum of still states remains a still state is non-overlapping of the long edges (see Lemma 5 below): if a particular edge is long in the first state, then it should be short in the second state, and visa versa.

From this we deduce that the building block should have low concentrations of long edges, and the placement of these edges should be localized as highly as possible. If both of these requirements are satisfied, one can add together shifted copies of the building block to generate new still states with higher concentrations.

Lemma 5. *The sum $\boldsymbol{\kappa}_1 + \boldsymbol{\kappa}_2$ of two still states $\boldsymbol{\kappa}_1$ and $\boldsymbol{\kappa}_2$ is a still state provided $\boldsymbol{\kappa}_1 \cdot \boldsymbol{\kappa}_2 = 0$.*

Proof. Since $\boldsymbol{\kappa}_1$ and $\boldsymbol{\kappa}_2$ are still states, their components satisfy

$$(\boldsymbol{\kappa}_1)_{ij} \in \{0, s\}, \quad (\boldsymbol{\kappa}_2)_{ij} \in \{0, s\}$$

for all connected nodes i and j. Moreover, the condition of orthogonality $\boldsymbol{\kappa}_1 \cdot \boldsymbol{\kappa}_2 = 0$ says that for

each pair (i,j) the values $(\boldsymbol{\kappa}_1)_{ij}$ and $(\boldsymbol{\kappa}_2)_{ij}$ cannot equal s simultaneously. Thus,

$$(\boldsymbol{\kappa}_1)_{ij} + (\boldsymbol{\kappa}_2)_{ij} \in \{0, s\}$$

Also, since $\boldsymbol{\kappa}_1$ and $\boldsymbol{\kappa}_2$ are still states, we have

$$Z\boldsymbol{\kappa}_1 = 0, \quad Z\boldsymbol{\kappa}_2 = 0,$$

where Z is the matrix of the hexagonal system (6.70). By linearity Z,

$$Z(\boldsymbol{\kappa}_1 + \boldsymbol{\kappa}_2) = Z\boldsymbol{\kappa}_1 + Z\boldsymbol{\kappa}_2 = 0$$

Since the necessary conditions hold, the sum $\boldsymbol{\kappa}_1 + \boldsymbol{\kappa}_2$ is a still state.

□

Notice that Lemma 5 states that sum

$$\boldsymbol{\kappa}_1 + \boldsymbol{\kappa}_2 + \ldots + \boldsymbol{\kappa}_m$$

is a still state, provided $\boldsymbol{\kappa}_i$, $i = 1, \ldots, m$ have non-overlapping long edges.

For a still state in (6.68) we have $||\boldsymbol{k}_e||_2 \leq s$. Thus

$$\left\| \mathrm{m}\left(\frac{1}{|\mathcal{T}|} Q^{-1} \sum_{e \in \mathcal{E}_B} \boldsymbol{k}_e \right) \right\|_F \leq \sqrt{2} \frac{|\mathcal{E}_B|}{|\mathcal{T}|} ||Q^{-1}||_2 s \tag{6.73}$$

Define concentrations α_i, $i \in \{1,2,3\}$, of long edges in a still state as the ratio of the long edges in i-th direction to the total number of all edges in this direction. Using the concentrations we can state the main result of this chapter: The set of still states concentrations densely fills a cube in $\mathbb{R}^3$. This result is proved in the following theorem.

Theorem 5. *For any $\alpha_i \in [0,1]$, $i = 1,2,3$, and any $n \geq 3$ there exists a still state $\boldsymbol{\kappa}^*$ such that its concentrations α_i^*, $i = 1,2,3$, satisfy*

$$|\alpha_i - \alpha_i^*| < \frac{1}{n}$$

Proof. To prove the theorem we will use special still states called *stripes*. These states have $\boldsymbol{\kappa}_{ij} = 0$ everywhere except for one stripe that has non-zero elements in one direction (figure 6.14). We can see that these stripes are still states because their components are either 0 or s and they satisfy the hexagonal equations: each hexagon has either all zero elongations or one non-zero inner elongation and one non-zero outer elongation.

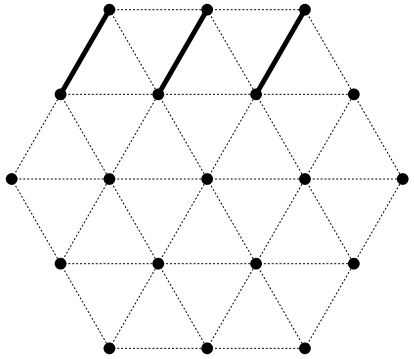

(a) A horizontal stripe, group 1

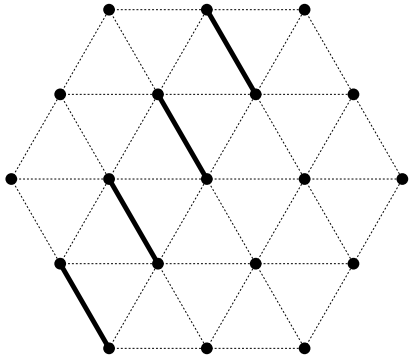

(b) Rotated stripe, group 2

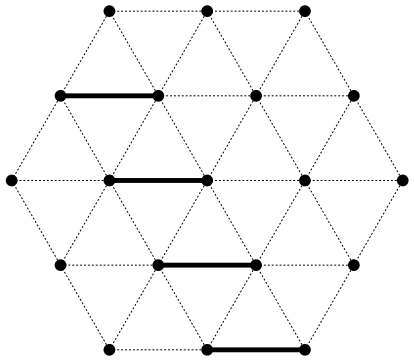

(c) Rotated stripe, group 3

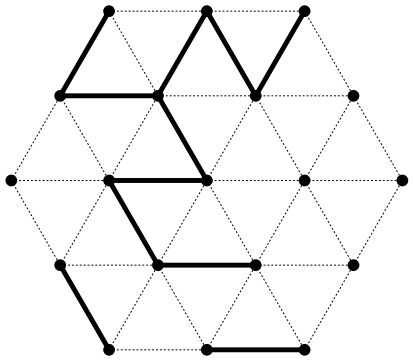

(d) Compound still state

Figure 6.14: 6.14(a), 6.14(b), and 6.14(b) are "stripe" still states. 6.14(d) is a still state composed of 6.14(a), 6.14(b), and 6.14(c). Solid line corresponds to $\kappa = s$, dotted line is 0.

Observe, that for two different stripes $\boldsymbol{\kappa}_1$ and $\boldsymbol{\kappa}_2$ we have $\boldsymbol{\kappa}_1 \cdot \boldsymbol{\kappa}_2 = 0$. In other words, the long edges of $\boldsymbol{\kappa}_1$ do not overlap the long edges of $\boldsymbol{\kappa}_2$, and thus $\boldsymbol{\kappa}_1 + \boldsymbol{\kappa}_2$ is a still state (figure 6.14(d)).

We have 3 different groups of stripes, $\mathcal{G}_1$, $\mathcal{G}_2$, and $\mathcal{G}_3$, one for each direction: one group of horizontal stripes and two groups of rotated stripes. The number of stripes in each group is $2(n-1)$.

Next, define the vectors $\boldsymbol{d}_r$, $r \in \{1,2,3\}$ as follows. The dimension of $\boldsymbol{d}_r$ is E (the number of edges), and the components are equal to one if the corresponding edge is parallel to $\boldsymbol{q}_r$ (a lattice direction vector), and equal to zero otherwise. It is easy to see that if $\boldsymbol{\kappa} \in \mathcal{G}_r$ for some $r \in \{1,2,3\}$ then $\boldsymbol{\kappa} \cdot \boldsymbol{d}_r < 2n$, $r = 1,2,3$, since each "stripe" has no more than $2n$ long edges. Also, since each stripe has long edges only in r-th direction, we get

$$\boldsymbol{\kappa} \cdot \boldsymbol{d}_r = \frac{E}{3}\alpha_r, \quad \boldsymbol{\kappa} \cdot \boldsymbol{d}_t = 0 \text{ for } t \neq r.$$

This implies

$$\alpha_r < \frac{6n}{E} = \frac{6n}{9n^2 - 15n + 6} < \frac{1}{n} \text{ for } n \geq 3.$$

First, we explain the main idea of the proof. Consider i-th group (stripes of one certain direction). If we add all stripes of this group then we'll get $\alpha_i = 1$. For the still state $\boldsymbol{\kappa} = 0$ we have $\alpha_i = 0$. Therefore, adding stripes one by one we increase α_i from 0 to 1 with steps less than n^{-1}. Hence, for any $x \in [0,1]$ there exists a step when $|\alpha_i - x| < n^{-1}$. Finally, since different directions are independent from each other, we can run this algorithm for $i = 1,2,3$ and at the end add all still states together to get what we need. Next, we present the technical details.

For any subset $\mathcal{S}$ of set $\mathcal{G}_i$ we will define functions $\hat{\boldsymbol{\kappa}}(\mathcal{S})$ and $\hat{\alpha}_j(\mathcal{S})$ by

$$\hat{\boldsymbol{\kappa}}(\mathcal{S}) = \sum_{\boldsymbol{\kappa} \in \mathcal{S}} \boldsymbol{\kappa} \quad \text{and} \quad \hat{\alpha}_j(\mathcal{S}) = \sum_{\boldsymbol{\kappa} \in \mathcal{S}} \frac{3}{E} \boldsymbol{\kappa} \cdot \boldsymbol{d}_j = \frac{3}{E} \hat{\boldsymbol{\kappa}}(\mathcal{S}) \cdot \boldsymbol{d}_j$$

Since $\hat{\boldsymbol{\kappa}}(\mathcal{G}_i) = \boldsymbol{d}_i$, we have $\hat{\alpha}_i(\mathcal{G}_i) = 1$ and $\hat{\alpha}_j(\mathcal{G}_i) = 0$ for $j \neq i$. Also, we define $\hat{\boldsymbol{\kappa}}(\emptyset) = 0$ and $\hat{\alpha}_j(\emptyset) = 0$, $j = 1,2,3$.

From the corollary of lemma 5 it follows that for any $\mathcal{S} \subset \mathcal{G}_i$ the value of function $\hat{\boldsymbol{\kappa}}(\mathcal{S})$ is a still state with concentrations $\hat{\alpha}_j(\mathcal{S})$.

Suppose we are given values $\alpha_i \in [0,1]$, $i = 1,2,3$. Let's define sets $\mathcal{H}_i$, $i = 1,2,3$, as

$$\mathcal{H}_i = \{\mathcal{S} \subset \mathcal{G}_i : \hat{\alpha}_i(\mathcal{S}) \leq \alpha_i\}$$

Having defined $\mathcal{H}_i$ we define values $\mathcal{S}_i^*$, $i = 1, 2, 3$, by

$$\mathcal{S}_i^* = \underset{\mathcal{S} \in \mathcal{H}_i}{\text{argmax}}\ \hat{\alpha}_i(\mathcal{S})$$

Since the sets $\mathcal{G}_i$ are finite, the sets $\mathcal{H}_i$ are finite and the maximum exists. Therefore, the definition of $\mathcal{S}_i^*$ is consistent.

Now if for some $i \in \{1, 2, 3\}$ we have $\mathcal{G}_i \backslash \mathcal{S}_i^* = \emptyset$ then $\mathcal{S}_i^* = \mathcal{G}_i$ and $\hat{\alpha}(\mathcal{S}_i^*) = 1$. From the definition of $\mathcal{S}_i^*$ we have

$$\hat{\alpha}_i(\mathcal{S}_i^*) \leq \alpha_i$$

Since $\alpha_i \leq 1$, we get $\hat{\alpha}_i(\mathcal{S}_i^*) = \alpha_i$.

If for some $i \in \{1, 2, 3\}$ we have $\mathcal{G}_i \backslash \mathcal{S}_i^* \neq \emptyset$ then there exists $\boldsymbol{k} \in \mathcal{G}_i \backslash \mathcal{S}_i^*$.

From the definition of function $\hat{\alpha}$ we get

$$\hat{\alpha}(\mathcal{S}_i^* \cup \{\boldsymbol{k}\}) = \hat{\alpha}(\mathcal{S}_i^*) + \hat{\alpha}(\{\boldsymbol{k}\}) > \hat{\alpha}(\mathcal{S}_i^*)$$

And, since $\mathcal{S}_i^*$ has maximal value in $\mathcal{H}_i$, we have $\mathcal{S}_i^* \cup \{\boldsymbol{k}\} \notin \mathcal{H}_i$. Hence,

$$\alpha_i < \hat{\alpha}_i(\mathcal{S}_i^* \cup \{\boldsymbol{k}\})$$

Now using

$$\hat{\alpha}_i(\mathcal{S}_i^*) \leq \alpha_i < \hat{\alpha}_i(\mathcal{S}_i^* \cup \{\boldsymbol{k}\})$$

and

$$\hat{\alpha}_i(\mathcal{S}_i^* \cup \{\boldsymbol{k}\}) - \hat{\alpha}_i(\mathcal{S}_i^*) = \hat{\alpha}_i(\{\boldsymbol{k}\}) < \frac{1}{n}$$

we get

$$0 \leq \alpha_i^* - \hat{\alpha}_i(\mathcal{S}_i^*) < \hat{\alpha}_i(\mathcal{S}_i^* \cup \{\boldsymbol{k}\}) - \hat{\alpha}_i(\mathcal{S}_i^*) < \frac{1}{n}$$

Finally, for the still state $\boldsymbol{\kappa}^*$ defined by

$$\boldsymbol{\kappa}^* = \hat{\boldsymbol{\kappa}}(\mathcal{S}_1^* \cup \mathcal{S}_2^* \cup \mathcal{S}_3^*)$$

we have

$$|\alpha_i^* - \alpha_i| < \frac{1}{n}$$

□

Let us define the set $\mathcal{D}$:

$$\mathcal{D} = \{s\,\mathrm{m}(Q^{-1}\boldsymbol{x}) : \boldsymbol{x} \in \mathbb{R}^3, 0 \le x_r \le 1, r = 1, 2, 3\}, \tag{6.74}$$

where Q^{-1} is the inverse of the matrix given by Eq. (6.64). Set $\mathcal{D}$ is a convex polygon in the space of 2×2 symmetric matrices, since it is an image of a cube under a non-singular linear transformation. The components of the elements of $\mathcal{D}$ form a set shown on figure 6.15.

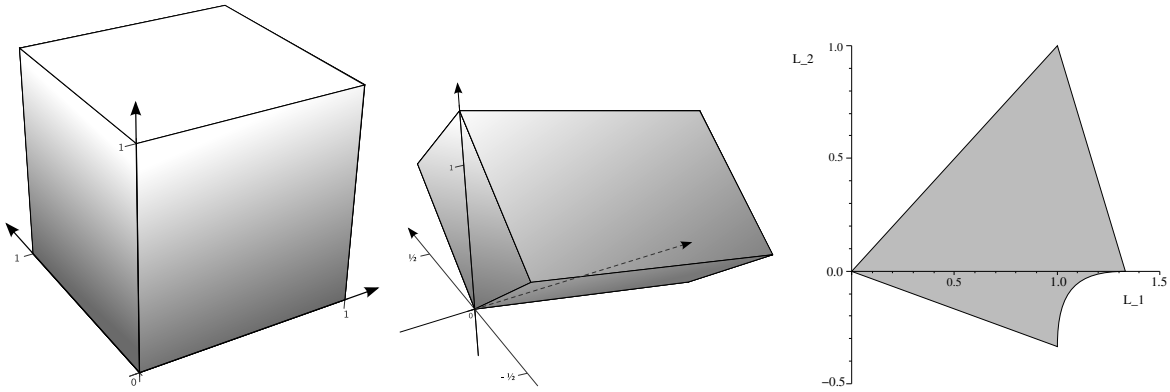

(a) The cube $[0, 1]^3$ (b) $Q^{-1}[0, 1]^3$ (c) Eigenvalues of $\bar{E}$

Figure 6.15: The cube and its image under Q^{-1}

Theorem 6. *For any $\boldsymbol{E} \in \mathcal{D}$ there exists a still state of the hexagonal array with a side of $n \ge 3$ points such that average strain $\boldsymbol{E}^*$ of this still state satisfies*

$$||\boldsymbol{E}^* - \boldsymbol{E}||_F \le s||Q^{-1}||_2 \frac{8}{n-1}$$

Proof. Since $\boldsymbol{E} \in \mathcal{D}$, there exists $\boldsymbol{\alpha} \in \mathbb{R}^3$, $0 \le \alpha_r \le 1$, such that

$$\boldsymbol{E} = s\,\mathrm{m}(Q^{-1}\boldsymbol{\alpha})$$

Using theorem 5 we can claim that for $n \ge 3$ there is a still state with the concentration values $\boldsymbol{\alpha}^*$

such that

$$||\boldsymbol{\alpha}^* - \boldsymbol{\alpha}||_2 \leq \frac{\sqrt{3}}{n}$$

Using (6.67), for this still state we find the average eigenstrain

$$\boldsymbol{E}^* = 2\frac{|\mathcal{E}|}{|\mathcal{T}|}\,\mathrm{m}(Q^{-1}\bar{\boldsymbol{k}}^*) - \frac{1}{|\mathcal{T}|}\,\mathrm{m}(Q^{-1}\sum_{e\in\mathcal{E}_B}\boldsymbol{k}_e^*).$$

Then

$$\begin{aligned}
||\boldsymbol{E}^* - \boldsymbol{E}||_F &= \left\| 2\frac{|\mathcal{E}|}{|\mathcal{T}|}\,\mathrm{m}(Q^{-1}\bar{\boldsymbol{k}}^*) - \frac{1}{|\mathcal{T}|}\,\mathrm{m}(Q^{-1}\sum_{e\in\mathcal{E}_B}\boldsymbol{k}_e^*) - \boldsymbol{E}\right\|_F \\
&= \left\| \frac{2s}{3}\frac{|\mathcal{E}|}{|\mathcal{T}|}\,\mathrm{m}(Q^{-1}\boldsymbol{\alpha}^*) - \frac{1}{|\mathcal{T}|}\,\mathrm{m}(Q^{-1}\sum_{e\in\mathcal{E}_B}\boldsymbol{k}_e^*) - s\,\mathrm{m}(Q^{-1}\boldsymbol{\alpha})\right\|_F \\
&\leq \sqrt{2}||Q^{-1}||_2 \left\| \frac{2s}{3}\frac{|\mathcal{E}|}{|\mathcal{T}|}\boldsymbol{\alpha}^* - s\boldsymbol{\alpha}\right\|_2 + \left\| \mathrm{m}\left(\frac{1}{|\mathcal{T}|}Q^{-1}\sum_{e\in\mathcal{E}_B}\boldsymbol{k}_e^*\right)\right\|_F
\end{aligned}$$

Next,

$$\begin{aligned}
\left\| \frac{2s}{3}\frac{|\mathcal{E}|}{|\mathcal{T}|}\boldsymbol{\alpha}^* - s\boldsymbol{\alpha}\right\|_2 &\leq s||\boldsymbol{\alpha}^* - \boldsymbol{\alpha}||_2 + s\left|1 - \frac{2}{3}\frac{|\mathcal{E}|}{|\mathcal{T}|}\right| ||\boldsymbol{\alpha}^*||_2 \\
&\leq \frac{\sqrt{3}}{n}s + s\left|1 - \frac{2}{3}\frac{|\mathcal{E}|}{|\mathcal{T}|}\right|\sqrt{3}
\end{aligned}$$

Further, using

$$|\mathcal{T}| = 6(n-1)^2, \quad |\mathcal{E}| = 9n^2 - 15n + 6, \quad |\mathcal{E}_B| = 6(n-1)$$

and estimation (6.73) we find

$$\begin{aligned}
||\boldsymbol{E}^* - \boldsymbol{E}||_F &\leq \sqrt{2}||Q^{-1}||_2\left(\frac{\sqrt{3}}{n}s + s\left|1 - \frac{2}{3}\frac{|\mathcal{E}|}{|\mathcal{T}|}\right|\sqrt{3}\right) + \sqrt{2}\frac{|\mathcal{E}_B|}{|\mathcal{T}|}||Q^{-1}||_2 s \\
&= \sqrt{2}s||Q^{-1}||_2\left(\frac{\sqrt{3}}{n} + \frac{\sqrt{3}}{3(n-1)} + \frac{1}{n-1}\right) \\
&\leq s||Q^{-1}||_2\frac{8}{n-1}
\end{aligned}$$

□

Let us now discuss the significance of the Theorem 6.3 for linking the microscopic (lattice-level) and macroscopic (continuum) models. First, it is of interest to understand how geometry of $\mathcal{D}$ depends on the microstructure. We observe that $\mathcal{D}$ is the image of a unit cube under a linear mapping defined in (6.74). The unit cube and the mapping m are both independent of the lattice geometry and the microscopic force definition. The two microstructure-dependent quantities in (6.74) are the relative (non-dimensional) critical elongation s and the matrix Q^{-1}. The actual critical elongation is sl, where l is the equilibrium edge length. Passing to the limit requires proper scaling of l with N (a typical scaling is $l \sim N^{-1/2}$). It looks natural to define s as a constant independent of N. If that is the case, then $s = O(1)$ as $N \to \infty$. The set $\mathcal{D}$ in that case is independent of N, and s is a non-dimensional constant of the problem that determines susceptibility of the material to phase transition. The diameter of $\mathcal{D}$ increases linearly with s. The matrix Q^{-1} determines orientation of $\mathcal{D}$ in the strain space and provides the explicit dependence of $\mathcal{D}$ on the lattice geometry. Indeed, by definition (6.64), Q depends only on the products of components of the lattice direction vectors $\boldsymbol{q}_r, r = 1, 2, 3$.

If $s = O(1)$, then $\mathcal{D}$ is the "flat bottom" of the macroscopic energy density, since by Theorem 6.3 any strain in this set can be approximated by a still state eigenstrain, the energy of every still state is zero, and $\mathcal{D}$ is fixed as $N \to \infty$.

CHAPTER SEVEN

CONCLUSION

A new complex continuum quantity $Q_\eta^\tau(t;\boldsymbol{x},\boldsymbol{z})$ was studied in this dissertation. The quantity is a function with derivatives bounded independently of N, it includes both velocities and positions of particles, and, hence, carries more information than the standard quantities density $\rho_\eta^\tau(t;\boldsymbol{x})$, linear momentum $\boldsymbol{p}_\eta^\tau(t;\boldsymbol{x})$, and kinetic energy $K_\eta^\tau(t;\boldsymbol{x})$. The standard quantities can be obtained from $Q_\eta^\tau(t;\boldsymbol{x},\boldsymbol{z})$.

Practical usage of $Q_\eta^\tau(t;\boldsymbol{x},\boldsymbol{z})$ was studied on several examples. Based on the examples we proposed a way to turn the evolution equation for $Q_\eta^\tau(t;\boldsymbol{x},\boldsymbol{z})$ into a closed form differential equation. This closure is exact under certain constraints and can be used as an approximation if the constraints are not satisfied. An algorithm is developed based on the presented closed form differential equation.

In the last chapter we proposed an example for further studies using $Q_\eta^\tau(t;\boldsymbol{x},\boldsymbol{z})$. The example is a bistable material modeled by a triangular lattice with bistable links. The equilibria of this triangular lattice are considered. We obtain the description of the set of the average strain tensors corresponding to still states, e.g. deformations that carry no forces and possess zero energy. We also propose several explicit constructions of such states for small and finite deformations.

The compatibility conditions for rod elongations were derived. In the small deformation case, these conditions are necessary and sufficient for the existence of a deformation realizing a given set of elongations. We propose a special class of still states, the strips. The strains of these special patterns densely cover the neutral region $\mathcal{D}$ of all still states strains. We showed that $\mathcal{D}$ is a parallelepiped in 3D space of independent components of the strain tensor. The orientation and side lengths of $\mathcal{D}$ are explicitly described in terms of the parameters of the lattice.

The above results suggest the following properties of the energy density: If a strain is inside of $\mathcal{D}$, then the energy density is asymptotically close to zero as the number of the lattice nodes approaches infinity; if the strain is outside of this set, the energy density is proportional to the square of the distance between the strain and $\mathcal{D}$.

Bibliography

[1] N. Ansini, A. Braides, and V. Chiadó Piat, *Interactions between homogenization and phase-transition processes*, Tr. Mat. Inst. Steklova **236** (2002), 373–385.

[2] N. Ansini, A. Braides, and V. Chiado‘ Piat, *Gradient theory of phase transitions in inhomogeneous media.*, Proc. Roy. Soc. Edin. A **133** (2003), 265–296.

[3] K. A. Ariyawansa, L. Berlyand, and A. Panchenko, *A network model of geometrically constrained deformations of granular materials*, Networks and Heterogeneous Media **3 (1)** (2008), 125–148.

[4] Katalin Bagi, *Stress and strain in granular asseblies*, Mechanics of Materials **22** (1996), 165–177.

[5] A. Cherkaev, E. Cherkaev, and L. Slepyan, *Transition waves in bistable structures i: Delocalization of damage ii: Analytical solution, wave speed, and energy dissipation*, J. Mech. Phys. Solids **53/2** (2005), 383–436.

[6] A. Cherkaev, V. Vinogradov, and S. Leealavanichkul, *The waves of damage in elastic lattices with waiting links*, Design and Simulation Mechanics of Materials **38** (2006), 748–756.

[7] A. Cherkaev and L. Zhornitskaya, *Protective structures with waiting links and their damage elovulion*, Multibody System Dynamics **13** (2005), 53–67.

[8] Andrej Cherkaev and Liya Zhornitskaya, *Dynamics of damage in two-dimensional structures with waiting links in: Asymptotics, singularities and homogenisation in problems of mechanics*, Kluwer (2004), 273–284.

[9] W. E and P.B. Ming, *Cauchy-Born rule and the stability of crystalline solids: static problems*, Arch. Ration. Mech. Anal. **183** (2007), 241–297.

[10] R. J. Hardy, *Formulas for determining local properties in molecular-dynamics simulations - shock waves*, Journal of Chemical Physics **76** (1982), 622–628.

[11] Lev Landau and Evgeny Lifshitz, *Statistical physics*, Pergamon Press, 1980.

[12] A. E. H. Love, *A treatise on the mathematical theory of elasticity*, New York Dover Publications, 1977.

[13] A. I. Murdoch and D. Bedeaux, *Continuum equations of balance via weighted averages of microscopic quantities*, Proc. R. Soc. Lond. A **445** (1994), 157–179.

[14] A. Ian Murdoch, *A critique of atomistic definitions of the stress tensor*, Journal of Elasticity **88** (2007), 113–140.

[15] M. Sataki, *Tensorial form definitions of discrete-mechanical quantities for granular assemblies*, International Journal of Solids and Structures **41** (2004), 5775–5791.

[16] Erwin Schrdinger, *Statistical thermodynamics*, Courier Dover Publications, 1989.

[17] L. I. Slepyan and M. V. Ayzenberg-Stepanenko, *Some surprising phenomena in weak-bond fracture of a triangular lattice*, J. Mech. Phys. Solids **50(8)** (2002), 1591–1625.

[18] ———, *Localized transition waves in bistable-bond lattices*, J. Mech. Phys. Solids **52** (2004), 1447–1479.

[19] Leonid Slepyan, Andrej Cherkaev, and Elena Cherkaev, *Transition waves in bistable structures. i. delocalization of damage*, Journal of the Mechanics and Physics of Solids **53** (2005), 383–405.

[20] ———, *Transition waves in bistable structures. ii. analytical solution: wave speed and energy dissipation*, Journal of the Mechanics and Physics of Solids **53** (2005), 407–436.

[21] L.I. Slepyan, *Feeding and dissipative waves in fracture and phase transition*, III. Triangular-cell lattice. J. Mech. Phys. Solids **49 (12)** (2001), 2839–2875.

[22] Leonid Splepyan, *Models and phenomena in fracture mechanics*, Sprnger-Verlag, 2002.

[23] C. Truesdell and W. Noll, *The non-linear field theories of mechanics*, In: Flügge, S (ed) Handbuch der Physik, vol. III/3. Springer, 1965.

[24] Lev Truskinovsky and Anna Vainchtein, *Kinetics of martensitic phase trasformations: lattice model*, SIAM Journ. Appl. Math. **66(2)** (2005), 533–553.

[25] ———, *Quasicontinuum models of dynamic phase transitions*, Continuum Mechanics and Thermodynamics **18** (2006), 1–21.

Appendix A

Mollification

Suppose that we have an expression

$$E = \frac{1}{N}\sum_{i=1}^{N} g(y_j)$$

for some smooth function $g : \mathbb{R}^n \to \mathbb{R}$. Let $K : \mathbb{R}^n \to \mathbb{R}$ be a positive valued function with bounded support:

$$K(y) \geq 0 \quad \text{for} \quad \forall y \in \mathbb{R}^n \qquad \operatorname{supp} K \subset B_r(0)$$

where $B_r(0)$ is a ball of radius r in $\|\cdot\|_2$ norm centered at 0 in $\mathbb{R}^n$. Also, assume that $\|K\|_{L_1(\mathbb{R}^n)} = 1$. Using K define K_δ:

$$K_\delta(y) = \frac{1}{\delta^n} K\left(\frac{y}{\delta}\right)$$

Note that $K_\delta(y) \geq 0$ and $\operatorname{supp} K_\delta \subset B_{r\delta}(0)$.

Consider the following approximation of E:

$$\tilde{E} = \int_{\mathbb{R}^n} g(y) \left\{ \frac{1}{N}\sum_{j=1}^{N} K_\delta(y - y_j) \right\} dv$$

Let us estimate the error of the approximation $|E - \tilde{E}|$:

$$\begin{aligned}
|E - \tilde{E}| &= \left| \int_{\mathbb{R}^n} g(y_j) \left\{ \frac{1}{N} \sum_{j=1}^{N} K_\delta(y - y_j) \right\} dy - \int_{\mathbb{R}^n} g(y) \left\{ \frac{1}{N} \sum_{j=1}^{N} K_\delta(y - y_j) \right\} dy \right| \\
&= \left| \int_{\mathbb{R}^n} (g(y) - g(y_j)) \left\{ \frac{1}{N} \sum_{j=1}^{N} K_\delta(y - y_j) \right\} dy \right| \\
&\leq \frac{1}{N} \sum_{j=1}^{N} \left| \int_{\mathbb{R}^n} (g(y) - g(y_j)) K_\delta(y - y_j) dy \right| \\
&= \frac{1}{N} \sum_{j=1}^{N} \left| \int_{B_{r\delta}(y_j)} (g(y) - g(y_j)) K_\delta(y - y_j) dy \right| \\
&\leq \frac{1}{N} \sum_{j=1}^{N} \sup_{B_{r\delta}(y_j)} |g(y) - g(y_j)| \int_{B_{r\delta}(y_j)} K_\delta(y - y_j) dy \\
&= \frac{1}{N} \sum_{j=1}^{N} \sup_{B_{r\delta}(y_j)} \left| (y - y_j) \cdot \int_0^1 \nabla g(sx + (1-s)y_j) ds \right| \\
&\leq \frac{1}{N} \sum_{j=1}^{N} r\delta \|g\|_{W^1_\infty} = r\delta \|g\|_{W^1_\infty(\mathbb{R}^n)}
\end{aligned}$$

Therefore,

$$\left| \frac{1}{N} \sum_{i=1}^{N} g(y_j) - \int_{\mathbb{R}^n} g(y) \mu_\delta(y) dy \right| \leq r\delta \|g\|_{W^1_\infty(\mathbb{R}^n)}$$

where

$$\mu_\delta(y) = \frac{1}{N} \sum_{j=1}^{N} K_\delta(y - y_j)$$